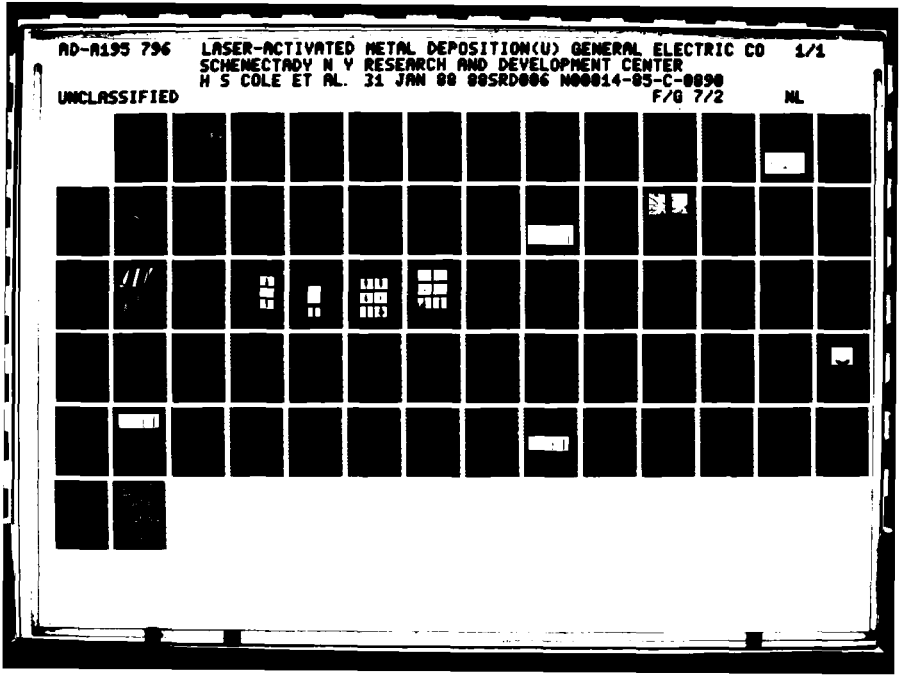
AD-A195 796 LASER-ACTIVATED METAL DEPOSITION(U) GENERAL ELECTRIC CO 1/1
SCHENECTADY N Y RESEARCH AND DEVELOPMENT CENTER
H S COLE ET AL. 31 JAN 88 88SRD006 N00014-85-C-0890
UNCLASSIFIED F/G 7/2 NL

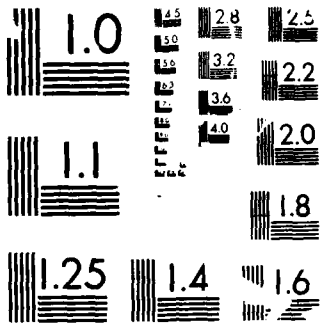

MICROCOPY RESOLUTION TEST CHART
NS 1963-A

(4)

88SRD006

LASER-ACTIVATED METAL DEPOSITION

Final Report

Prepared by

H.S. Cole, Y.S. Liu, R. Guida, J.W. Rose, and L.M. Levinson
General Electric Research and Development Center
Schenectady, New York 12345

Prepared for

U.S. Office of Naval Research/Strategic Defense Initiative Office
Contract No: N00014-85-C-0890
Period: October 1, 1985 to December 31, 1987

January 31, 1988

UNCLASSIFIED

SECURITY CLASSIFICATION OF THIS PAGE

REPORT DOCUMENTATION PAGE

1a. REPORT SECURITY CLASSIFICATION: unclassified	1b. RESTRICTIVE MARKINGS
2a. SECURITY CLASSIFICATION AUTHORITY	3. DISTRIBUTION/AVAILABILITY OF REPORT
2b. DECLASSIFICATION/DOWNGRADING SCHEDULE	
4. PERFORMING ORGANIZATION REPORT NUMBER(S): 88SRD006	5. MONITORING ORGANIZATION REPORT NUMBER(S)
6a. NAME OF PERFORMING ORGANIZATION: General Electric Company, Corporate Research & Development / 6b. OFFICE SYMBOL (If applicable)	7a. NAME OF MONITORING ORGANIZATION: Office of Naval Research
6c. ADDRESS (City, State and ZIP Code): P.O. Box 8, Schenectady, N.Y. 12301	7b. ADDRESS (City, State and ZIP Code): Materials Division, 800 N. Quincy Street, Arlington, Virginia 22217-5000
8a. NAME OF FUNDING/SPONSORING ORGANIZATION: SDI Office / 8b. OFFICE SYMBOL (If applicable)	9. PROCUREMENT INSTRUMENT IDENTIFICATION NUMBER: N00014-85-C-0890
8c. ADDRESS (City, State and ZIP Code): 1717 H St. N.W., Washington, D.C. 20006	10. SOURCE OF FUNDING NOS: PROGRAM ELEMENT NO. / PROJECT NO. / TASK NO / WORK UNIT NO.
11. TITLE (Include Security Classification): LASER ACTIVATED METAL DEPOSITION	
12. PERSONAL AUTHOR(S): H.S. Cole, Y.S. Liu, R. Guida, J. Rose, L. Levinson	
13a. TYPE OF REPORT: Final Technical Report / 13b. TIME COVERED: FROM 10/1/85 TO 12/31/87	14. DATE OF REPORT (Yr., Mo., Day): Jan. 31, 1988 / 15. PAGE COUNT: 56
16. SUPPLEMENTARY NOTATION	
17. COSATI CODES: FIELD / GROUP / SUB. GR.	18. SUBJECT TERMS (Continue on reverse if necessary and identify by block number)

19. ABSTRACT (Continue on reverse if necessary and identify by block number)

A process to selectively deposit copper on polyimide was developed. Laser irradiation of organometallic palladium compounds with a CW argon ion laser at 351 nm was used to selectively deposit catalytic amounts of palladium on polyimide. Subsequent immersion of the irradiated samples in an electroless copper solution resulted in selective copper deposition. Since only a few monolayers of palladium were needed to catalyze the electroless copper process, fast writing speeds of up to 10 cm/s were achieved. Copper lines with 1.5 μm thickness and resistivities of 3 mΩ-cm were produced by this technique.

20. DISTRIBUTION/AVAILABILITY OF ABSTRACT: UNCLASSIFIED/UNLIMITED ☐ SAME AS RPT ☐ DTIC USERS ☐	21. ABSTRACT SECURITY CLASSIFICATION: unclassified
22a. NAME OF RESPONSIBLE INDIVIDUAL: Dr. Robert C. Pohanka	22b. TELEPHONE NUMBER (Include Area Code): (202) 696-4401 / 22c. OFFICE SYMBOL: CODE 431N

DD FORM 1473, 83 APR EDITION OF 1 JAN 73 IS OBSOLETE

UNCLASSIFIED

SECURITY CLASSIFICATION OF THIS PAGE

Acknowledgment

This work was sponsored by the U.S. Office of Naval Research/Strategic Defense Initiative Office under Contract No. N00014-85-C-0890. The work was performed during the period of October 1985 to December 1987. The authors wish to acknowledge the contribution of Dr. H.R. Philipp for his measurements of VUV optical properties of polymers relevant to the present study and the contribution of Professor H. Bakhru of the Physics Department at the State University of New York at Albany, New York, for his assistance in the RBS measurements. Many helpful discussions with Dr. Brad Karas and Dr. Don Faust on various metallization processes are gratefully acknowledged. We also want to thank Dr. R.C. Pohanka and Dr. W. Smith of the Office of Naval Research for their management support throughout the course of this program.

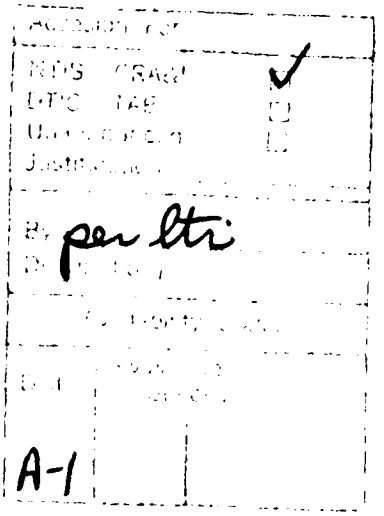

TABLE OF CONTENTS

TABLE OF CONTENTS (Cont'd)

LIST OF ILLUSTRATIONS

LIST OF TABLES

Section 1

SUMMARY

The objective of this program has been to investigate laser-activated chemistry for fabricating metal lines on low dielectric constant substrates in high-speed interconnect technology. A survey of laser-driven processes for metal deposition from organometallic compounds was completed, and potentially useful candidate materials were evaluated. Various approaches including gas phase and thin film deposition processes were investigated.

A process to selectively deposit copper on polyimide was developed. Laser irradiation of organometallic palladium compounds with a CW argon ion laser at 351 nm was used to selectively deposit catalytic amounts of palladium on polyimide. Subsequent immersion of the irradiated samples in an electroless copper solution resulted in selective copper deposition. Since only a few monolayers of palladium were needed to catalyze the electroless copper process, fast writing speeds of up to 10 cm/s were achieved. Copper lines with 1.5 μm thickness and resistivities of ? $\mu\Omega$-cm were produced by this technique.

The major accomplishments of this program were

- Investigated laser-activated metal deposition processes on low dielectric constant substrates for high-speed interconnection applications.
- Developed laser-activated copper deposition process on polyimide.
- Determined critical surface Pd concentration for optimum electroless copper deposition using the Rutherford Backscattering (RBS) technique.
- Demonstrated 7 μm to 50 μm wide copper lines to 1.5 μm thick with high conductivity (3$\mu\Omega$-cm) and excellent morphology.
- Demonstrated fast laser writing speeds up to 10 cm/s.

Section 2

INTRODUCTION AND PROGRAM OBJECTIVES

Polymeric materials are gaining acceptance for use in electronic packaging applications as the interlayer dielectric, passivation and planarization layer in multilevel interconnect processes (Refs. 1, 2, 3). These materials are inexpensive; they can be applied by a variety of coating techniques to any desired shape; they can withstand required solder temperatures; they have excellent dielectric strengths and low dielectric constants. For example, the values of ϵ for BeO ceramics are 6 to 8 and for Al_2O_3 ceramics about 8 to 10 as compared to 3 for polyimides. This low value of dielectric constants results in reduced capacitive coupling, which has a direct bearing on the ultimate speed or frequency of the packaged device. Further, reduced capacitive coupling allows the circuit designer to shrink the inter line spacing (pitch) thus reducing the overall package size.

Generally, standard metallization and photolithographic processes have been used to make interconnects and etch via holes for contacts from one metal layer to another. Laser-activated chemistry has also been shown to be a viable method to fabricate metal lines on various substrates (Refs. 4-7). The production of metal lines by laser-induced deposition techniques offers several advantages over other thin film deposition processes because the process is noncontact, maskless, low temperature, selective, and relatively simple.

Although a variety of laser processes and organometallic compounds have been studied, little attention has been given to laser metal deposition on polymeric substrates. These organic materials do not possess the same high thermal stability as previously studied inorganic materials and therefore new deposition parameters must be developed. To develop a viable laser-activated metallization process using this technologically important electronic material is the central focus of this program.

Therefor, the overall program objective was to investigate novel metallization processes using laser-activated chemistry to fabricate metal lines on polymeric substrates. Two general approaches were considered: (a) gas phase pyrolysis and photolysis of organometallic compounds, and (b) laser-induced decomposition of metal containing thin films or compounds. A review of known laser deposition processes and chemistry was conducted as a starting point for this research.

Section 3

TECHNICAL CONSIDERATIONS

3.1 Laser-Assisted Deposition Processes

There has been an increasing amount of interest and activity recently in the area of laser-assisted thin film deposition. For the interested reader, a review of these processes can be found in Refs. 5 and 6. Lasers of different type and wavelength have been used to deposit metals, insulators, and semiconducting materials. For this discussion, we will only be concerned with metal deposition processes. The advantage of laser processing is that it is selective, is low temperature, and has the added advantage of being adaptable to circuit design changes.

Several mechanisms have been studied as a means of depositing metal films on inorganic substrates: (a) photodissociation of organometallic compounds in the gas phase to locally deposit metal, (b) localized heating of the substrate to thermally decompose gas molecules and directly deposit metal, and (c) direct photolytic or pyrolytic decomposition of organometallic compounds or metal containing inks that have been coated as thin films on appropriate substrates. A few examples of direct write laser deposition processes are shown in Table 1.

In general, the growth rate of laser-activated deposition processes depends on beam intensity, wavelength, and the concentration of precursors. The exact nature of the reaction is also extremely important. In gas phase photolysis, growth rates are limited by the transport of reactants and products to and away from the reaction zone. The proper laser wavelength must be used in order to couple the spectral properties of the gaseous phase compounds for photodissociation with efficient quantum yield. Most organometallic compounds absorb UV between 200 and 400 nm. The gas phase absorbance spectra for candidate materials are listed in Appendix 1. The absorbance spectra for these compounds varied dramatically as did their photolytic stability. For example, metal alkyls such as dimethyl cadmium have been studied in detail by Anderson and Taylor (Ref. 13) and have been shown to dissociate at photon energies on the order of a few eV's. Metal carbonyls also photodissociate at these energy levels. However, dimethyl cadmium and chromium carbonyl exhibit much different deposition rates as shown in Table 1 which was attributed to the difference in absorbance as well as laser power. The major disadvantage of gas phase photolytic processes is that decomposition

Table 1

DIRECT WRITE LASER-METAL DEPOSITION PROCESSES

PROCESS	REACTION	DEPOSITION RATE	SCAN RATE
GAS PHASE PHOTOLYSIS	$Cd(CH_3)_2 \xrightarrow[257\ nm]{(CW)} Cd$	1 μm/s	TOO SLOW FOR LINE SCAN
	$Cr(CO)_6 \xrightarrow[308\ nm]{(PULSED)} Cr$	10^{-4} μm/s (10 Hz)	
THIN FILM PHOTOLYSIS	$Mn_2(CO)_{10} \xrightarrow[325\ nm]{(CW)} Mn(CO)_5$		
	$Mn(CO)_5 + Ag\ OTf \longrightarrow Ag$	10^{-3} μm/s	
GAS PHASE PYROLYSIS	$(CH_3)_2 Au(HFAc) \xrightarrow[514\ nm]{(CW)} Au$	6 μm/s	~ 1 mm/s
	$WF_6 + Si \xrightarrow[514\ nm]{(CW)} W$	100 μm/s	~ 1 mm/s
THIN FILM PYROLYSIS	$Au\text{-}ink \xrightarrow[514\ nm]{(CW)} Au$	DICTATED BY INITIAL FILM THICKNESS	0.2 mm/s

can occur in the gas phase as well as at the gas-substrate interface where an adsorbed layer of organometallic compound is present. At a given wavelength and laser power, the concentration of organometallic in the gas phase must be increased in order to achieve a fast deposition rate. This can result in additional gas phase dissociation and cause undesired particulate formation on the substrate. Additionally, high gas phase concentrations may result in deposition on the inner surface of the quartz window of the gas cell during irradiation. These factors limit the absolute growth rate for this process and make this an impractical approach for laser scanning processes.

In gas phase pyrolytic processes, reactants of higher concentration can be used because local heating of the substrate can occur without affecting the gas phase or cell window. As a result, a significant improvement in growth rates has been achieved. The key requirement for efficient deposition is that the substrate must be highly absorbing at the wavelength of irradiation.

At the initial phase of this program, we have investigated various compounds as possible reagents for metal deposition. A stainless steel gas cell fitted with a quartz window was used for these experiments (Figure 1). With this apparatus, organometallic precursor materials could be irradiated in a static or flowing gas environment. By heating the entire cell, carrier gases were used to control reactant concentrations. A list of compounds we have evaluated is shown in Table 2. One interesting reaction is the deposition of tungsten on silicon from tungsten hexafluoride (Ref. 7). High writing speeds were possible because of the catalytic reduction reaction between tungsten and silicon at elevated temperatures. This was a surface selective reaction since deposition only occurred on silicon and suggested the possibility of catalysis to improve deposition rates for scanning applications.

Thin films of metal containing inks or organometallic compounds can be applied to appropriate substrates using a variety of coating techniques. The advantage of this approach is that relatively simple apparatus is required to contain the reactants. Further, higher laser power can be used if the substrate is sufficiently stable. The major disadvantage of this approach is the contamination of the metal deposits with carbon resulting from decomposition of organic ligands or polymeric materials. Higher growth rates are again obtained with thermal processes as indicated in Table 1.

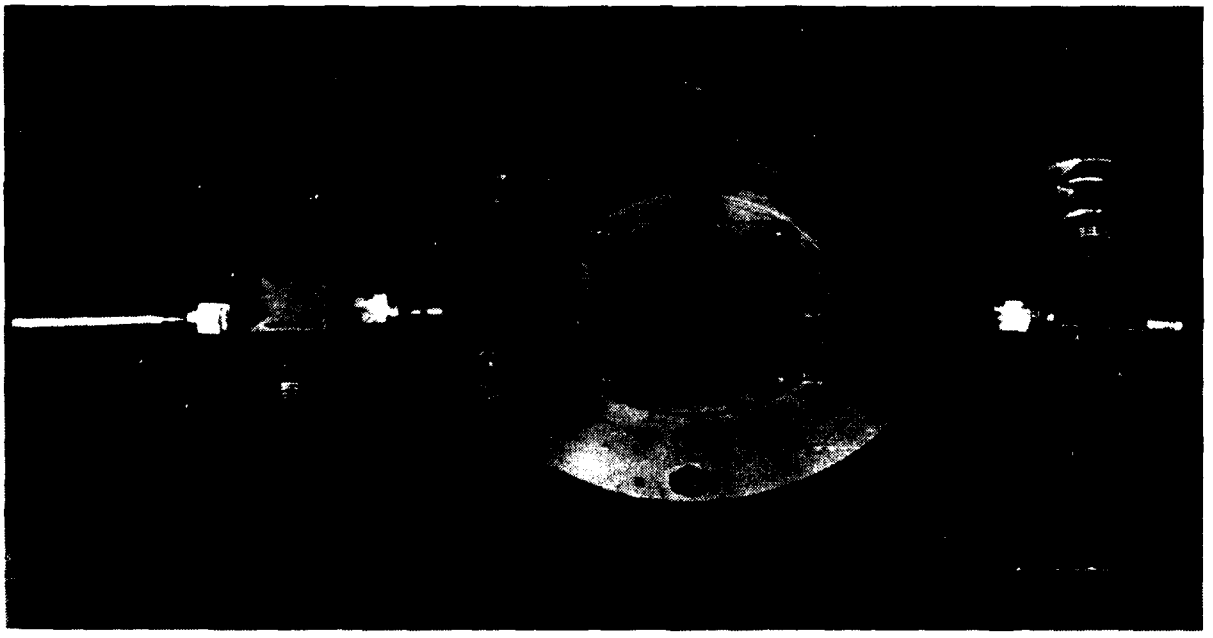

Figure 1. Stainless steel cell for gas phase laser deposition studies.

Table 2

ORGANOMETALLIC COMPOUNDS FOR LASER DEPOSITION EXPERIMENTS

	COMPOUND	REACTION	LASER WAVELENGTH (nm)	REMARKS
1.	TUNGSTEN CARBONYL	$W(CO)_6 \rightarrow W$	514,257 CW ARGON ION	— METAL DEPOSITED ON SILICON (514 nm) AND QUARTZ (257 nm)
2.	MOLYBDENUM CARBONYL	$Mo(CO)_6 \rightarrow Mo$	"	
3.	CHROMIUM CARBONYL	$Cr(CO)_6 \rightarrow Cr$	"	
4.	COPPER BIS HEXAFLUOROACETYL-ACETONATE	$Cu(C_5HO_2F_6)_2 \stackrel{\Delta}{\rightarrow} Cu$	514 CW	— Cu ON SILICON (514 nm) — NO DEPOSITS AT 257 nm
5.	CHROMIUM TRIS HEXAFLUOROACETYL-ACETONATE	$Cr(C_5HO_2F_6)_3 \rightarrow Cr$	514 CW 351 CW 193,248 PULSED EXCIMER	— Cr ON SILICON AND QUARTZ
6.	PALLADIUM BIS HEXAFLUOROACETYL-ACETONE	$Pd(C_5HO_2F_6)_2 \rightarrow Pd$	514,351,257 CW 193,248 PULSED EXCIMER	— PHOTOLYTIC AND PYROLYTIC DEPOSITIONS
7.	TUNGSTEN HEXAFLUORIDE	$WF_6 \rightarrow W$	514 CW	— DEPOSITION OF TUNGSTEN CATALYZED BY SILICON SURFACE — HIGH SPEED WRITING DEMONSTRATED

The overall body of literature on the topic of laser-induced metal deposition on various substrates has grown considerably over the last few years, although as stated earlier, laser deposition on polymeric materials has received little attention in the past and requires the development of new laser processes. For line scanning applications, fast deposition rates are required. From previous studies conducted at GE CRD, thermal processes have been shown to have higher deposition rates. These earlier experiments have been designed to deposit metals on inorganic substrates which have much higher thermal stability than those of organic polymeric materials. For example, chromium and copper were laser deposited on silicon from chromium carbonyl and copper hexafluoroacetylacetonate, respectively, by locally heating the surface with an argon ion laser at 514 nm. However, under the identical deposition condition using polyimide substrates, no deposition occurred. The power level was sufficiently high to cause decomposition of the polyimide as evidenced by charring and carbon residue. Deposition on polymeric substrates requires lower temperature processes than what has been reported to date.

3.2 Optical Considerations

Table 3 summarizes several critical requirements in applying the laser-induced CVD technique for metal deposition. These requirements are resolution, writing speed, resistivity, and surface morphology. Other considerations such as the cost and environmental considerations are also important in industrial applications. The resistivity of metal lines deposited by laser-induced CVD depends much upon composition, impurity and structure. The morphology of deposited structures are further affected by properties such as coherence effects, instability induced by beam nonuniformity, and chemical reactions involved. Here we consider the first two items that are critical to the optical considerations, namely, resolution and writing speed.

Table 3

REQUIREMENTS FOR LASER DIRECT WRITING

RESOLUTION	- Localization - Nonreciprocity
SPEED	- Rate of Reactions - Transport of Reactants
RESISTIVITY	- Composition - Impurity - Structure
MORPHOLOGY	- Coherence Effects - Nonuniform Heating - Instability

3.2.1 Resolution When a Gaussian laser beam is incident upon an absorbing substrate, local temperature rises as a result of absorption of the incident laser energy. A unique characteristic in laser-microchemical processing is the so-called "nonreciprocity" property caused by the strong nonlinear temperature dependence of the local reaction rate (Ref. 7). Depending upon the activation energy of the reactions employed, localization of the chemical reaction can result in an improvement of the writing resolution such that the structure produced is smaller than the diffraction-limited focussed spot size. To illustrate this effect, we plot in Figure 2 the temperature profiles induced by an argon ion laser at 415 nm with a Gaussian beam described as $I(r) = I_o \exp(-r^2/2r_o^2)$ with $r_o = 20\ \mu m$. The calculated relative chemical reaction rate, and the Gaussian laser beam profile, both normalized to the maximum surface temperature, are also drawn. The calculation assumed an Arrhenius-type rate with an activation energy of 0.5 eV. The figure shows the reaction is limited to a width less than the laser beam size.

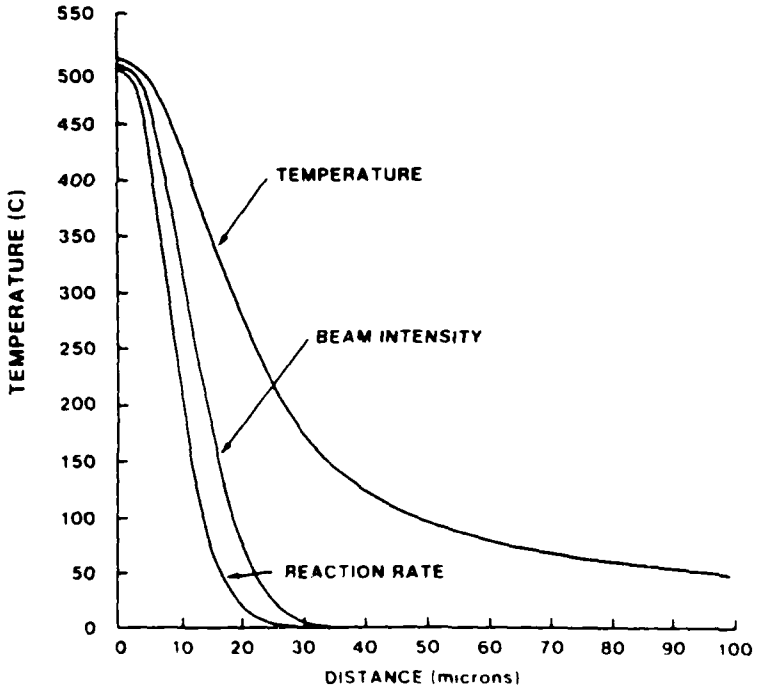

Figure 2. Temperature profile and reaction rate induced by a Gaussian laser beam. The substrate is a-Si (0.5 μm) on glass.

In the present work, the reaction rates are estimated to be less than 0.5 eV, the thermal conductivity of polymeric substrates is relatively small, and the improvement of resolution is not as pronounced. Figure 3 shows a calculation of the temperature profiles on a polyimide surface irradiated with an argon laser at 351 nm with a Gaussian intensity distribution. The various curves correspond to the temperature distributions for the laser beam scanned at 1 to 10 cm/s speeds, respectively, at a constant incident laser power of 20 mW. The maximum laser power is limited by the thermal decomposition of polyimide at about 550 to 600 °C.

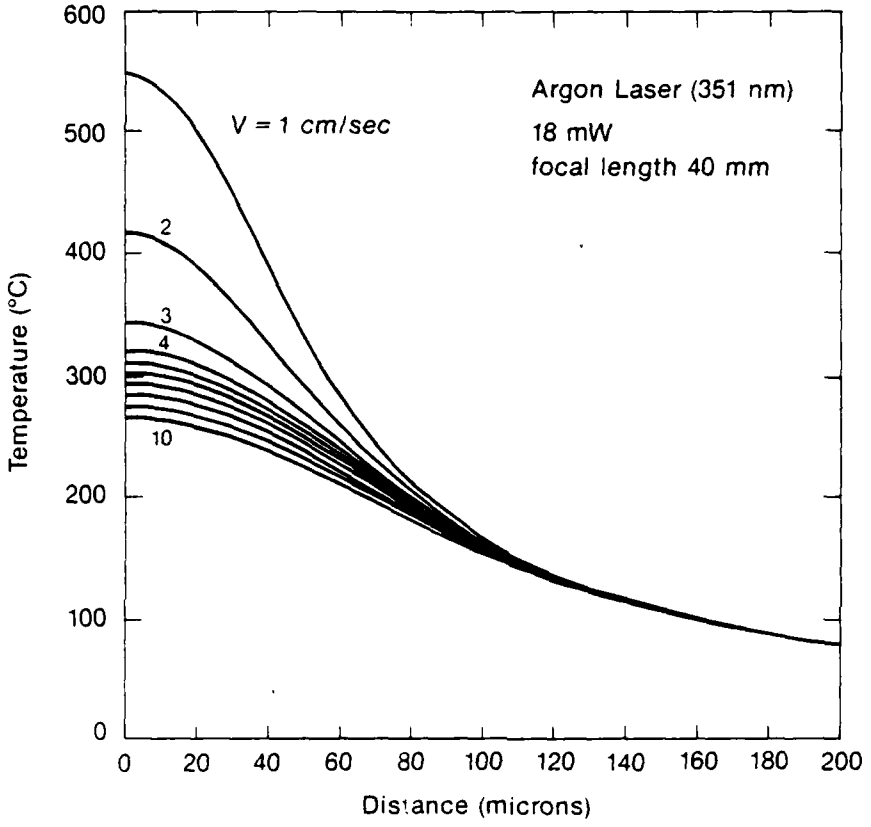

Figure 3. Temperature profiles of a Gaussian laser beam (351 mm) on polyimide

3.2.2 **Writing Speed** Another interesting property observed in a microchemical process using gas phase deposition induced by a laser source of micron dimension is the enhancement of the available reaction flux. The reaction rate in a heterogeneous reaction at a gas-solid interface is generally limited either by diffusion of reactants and/or products, or by reaction rates on the solid surface. The reactant flux channeled into the reaction zone increases at high pressure as the dimension of a reacting zone decreases to a value smaller as compared with the gas diffusion distance. On the other hand, for an extended heated surface, the reaction flux at a high pressure is usually limited by gas phase diffusion. From a geometrical scaling consideration, net reaction rates in a microchemical process induced by a focussed laser beam can be several orders of magnitude faster than those observed in a diffusion-limited case such as a furnace. For instance, a reaction flux of $1.0 \times 10^{21} cm^{-3}$ is available at a pressure of 100 torr for a 10 μm focussed Gaussian beam. The reaction flux reduces to a value of $1.0 \times 10^{19} cm^{-3}$ for a Gaussian beam of 1 mm dimension (Ref. 14).

The writing speed in a laser-induced CVD process can be explained using a simple model shown in Figure 4 in which D is the beam diameter, d the film thickness, V_g the film growth velocity, and V_s is the writing speed. The values of D and d are dictated by considerations such as resolution, and resistivity required for a given application. The growth velocity V_g depends upon types of reaction, temperature at which reactions take place, and the mass transport discussed earlier.

For packaging applications, a total of 1,000 to 2,000 interconnects are required with an average length of a few cm and suggests that a fast writing speed of ~cm/s is required. To achieve this writing speed, a growth velocity of ~100 μm/s is required for lines 12 μm wide.

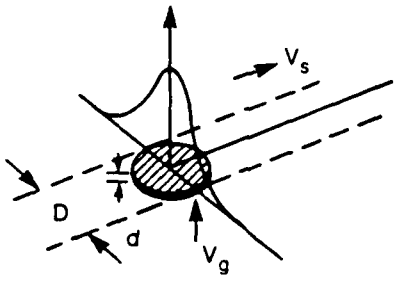

where:

$$V_s = \frac{D}{d} V_g$$

V_s = Scanning Speed

V_g = Growth Velocity

D = Beam Diameter

d = Film Thickness

Figure 4. A schematic to illustrate laser writing speed.

3.3 Organometallic Compounds

Most volatile organometallic compounds are either toxic or pyrophoric and must be used in a controlled environment. This is particularly true for metal alkyls and carbonyls of metals of interest for this work. An interesting series of compounds has been described by Wolf et al. (Ref. 15). These acetylacetonates are characterized by relatively high vapor pressures at room temperature. One such compound, copper hexafluoro acetylacetonate (CuHFAcAc), was synthesized by Houle and coworkers (Ref. 16), and evaluated as a precursor material for laser deposition of copper. They were able to laser deposit copper in the gas phase using an argon ion laser at 514 nm on silicon substrates. Typical deposition rates were about 1 μm/s at power levels of 10^5 W/cm^2 (Ref. 17). The advantage of this class of organometallic compounds is that they have much lower toxicity than the metal alkyls or carbonyls.

The copper, palladium, chromium, and aluminum hexafluoro acetylacetonate compounds were synthesized and evaluated as candidate materials for laser metal deposition on polyimide during this program (see Appendix 2). These compounds could be thermally decomposed at temperatures between 200 and 300 °C. Deposits were observed on silicon at 514 nm, but irradiation at 257 nm with a frequency doubled argon ion laser showed no or little deposition even though the organometallics were absorbed in this region of the spectrum. In the case of the copper and palladium compound, we were

able to deposit metal when the compounds were irradiated with a mercury vapor lamp, suggesting that some photochemistry was possible with the compounds.

These compounds offered the promise of tailoring the reactivity and vapor pressure of the organometallic by appropriate molecular engineering. Various derivatives of these compounds could be synthesized with different organic ligands attached to the metal atom to alter the specific physical properties. For example, the generalized structure in Figure 5 shows the variation in molecular structure possible. Some of these derivatives are commercially available and will be described herein.

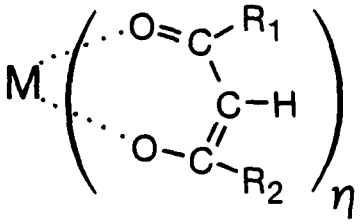

M = Pd, Cu, Cr, Al

R_1, R_2 = CH_3, C_2H_5, CF_3, OCH_3, $OCOCH_3$, etc.

Figure 5. Generalized structure of organometallic compounds.

3.4 Packaging Material Considerations

Polymers for electronic packages should have the following characteristics:

- low dielectric constant
- good adhesion
- solvent and moisture resistance
- dimensional stability
- thermal stability
- processability

Of the commercially available polymers, polyimide appears to have superior performance for packaging applications. The synthetic route to a typical polyimide is shown in Figure 6. A commercially available polyimide material is commonly known as Kapton (™DuPont Chemicals) and is available as a thin sheet or in solution form. The latter is in the amide-acid form and is soluble in solvents and is applicable in using spin-coating or spraying techniques. After baking at elevated temperature, the polymer converts to the imide form and it becomes virtually insoluble in organic solvents. The Kapton film (as received) is fully cured to the imide structure and can only be applied by lamination techniques. Numerous polyimides are available with different molecular structure and correspondingly different physical properties. For this work we chose to use the Du Pont polyimide (PMDA-ODA) shown in Figure 6 because of its broad acceptance for insulation applications in the electronic industry and also it was the material used in a current ongoing CRD program on High Density Interconnect Technology. This material has a glass transition temperature in excess of 400 °C and a dielectric constant of 3.3.

Low contact resistance and high conductivity are required for high-speed interconnect metallization. Because of its low bulk resistivity of 1.55 μ-Ω-cm, copper is the metal of choice for the current program.

Since the UV optical properties of polymers are important for the present work, we have investigated and measured the optical properties of a variety of polymeric materials described in Appendix 3.

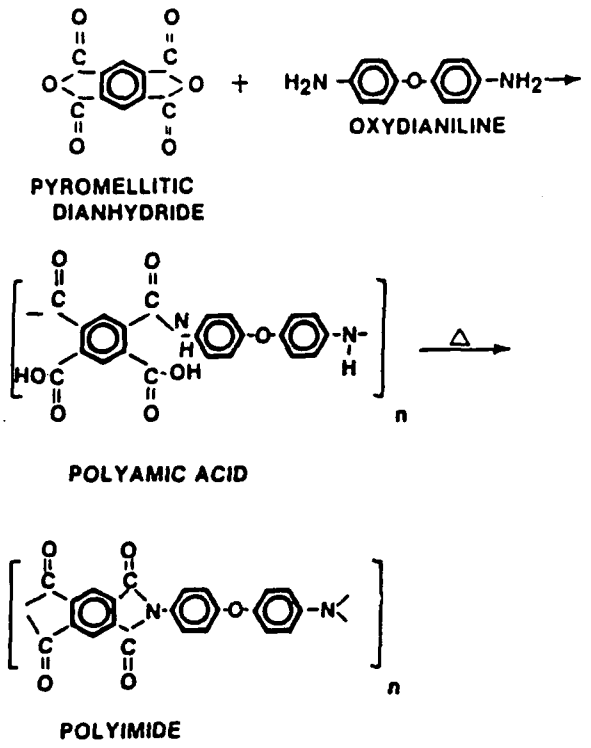

Figure 6. Synthesis and structure of Kapton™ polyimide

Section 4

EXPERIMENTAL RESULTS

4.1 Experimental Facility

4.1.1 Laser Direct Writing Facility All the laser processing work for this program was carried out at the advanced Laser Processing Facility, which was developed specifically for electronic materials fabrication. The facility includes a 15 W CW argon-ion laser, 0.4 W UV Argon Laser, a 15 W CW Nd:YAG laser, and a multigas excimer laser. The YAG laser is operable in either CW or pulsed Q-switched mode at 1.06, 0.53,and 0.26 μm.

4.1.2 Visible Argon Laser System The visible argon ion laser is a Spectral Physics model 171 multiple-line, 15 W average power laser, and is equipped with a littrow prism for single-line operation. The 514-nm output has been frequency-doubled to provide a CW UV source at 257 nm using a temperature-tuned KDP crystal. About 10 mW output has been generated and used for photo-induced chemical deposition of various metal lines.

4.1.3 UV Argon Laser System In addition, a UV argon laser (Spectral Physics Model 2205) was set up for the present program. The laser has an UV output of 0.4 W operated at multi-UV lines between 351 nm and 363 nm, or can be operated at single UV line selected by an intracavity dispersive prism. For the bulk of the present program, the UV argon laser at 351 nm was used, because polyimide absorbs strongly at this wavelength with an absorption coefficient of $>10^4$ cm^{-1}. This laser is also the only CW laser available which provides high power (below 400 nm) for fast scanning applications.

The laser systems are controlled from an IBM PC/XT computer system. The computer controls laser power, power on/off, scanning speed, and *xy* position of the sample.

4.1.4 YAG Laser System The YAG laser is a CW-pumped, acousto-optically Q-switched unit operable in three different modes: CW, pulsed at 1.06 μm, 0.53 μm, and 0.26 μm. In the CW operation, an average power of 20 W in TEMoo mode, and 150 W in multimode have been generated. In the Q-switched operation, an average power of 12 W at a pulse repetition rate of 5 KHz in TEMoo has been achieved with a pulse width of 140 ns. Intracavity doubling has generated 2 W using a $LiIO_3$ crystal, and 6 W using a KTP crystal (Ref. 25). The UV frequency quadrupling was operated using a temperature-tuned KDP crystal with an output of 50 mW at 266 nm (Ref. 26). The UV frequency-quadrupled output was used for laser-decomposed Pd from Pd containing organometallic compounds using photochemically induced decomposition.

4.1.5 Excimer Laser System The excimer laser system consists of a Lambda Physik Model EMG 150ET excimer laser operated at 193, 248, 308, and 351 nm of the ArF, KrF, XeCl, and XeF laser line, respectively. The laser is operable to 20 Hz with an average power of 2 W at 248 nm. The excimer laser consists of an oscillator and an amplifier, so it can be operated in either injection-locking mode to obtain line-narrowed, low divergence output, or in a power oscillator and power amplifier mode to increase the laser output.

4.1.6 *X-Y* Positioning System The laser systems are controlled from an IBM PC/XT computer system. The computer controls laser power, power on/off, scanning speed, and *x-y* position of the sample. The high resolution table, an Anorad II system supplied by the Anorad Corporation, provides a closed-loop servomotor-controlled positioner using a CMOS bus and logic system to provide high noise immunity. The micro-based *x-y* positioning system includes programmed functions such as linear interpolation, curve linear interpolation, programmable jog, dwell, and scan-and-repeat functions. The *X-Y* positioning table is mounted on a granite slab and employs optical encodes to achieve a resolution of 1 μm with a single repeatedly of 1 μm over 10 by 10-cm translation distance.

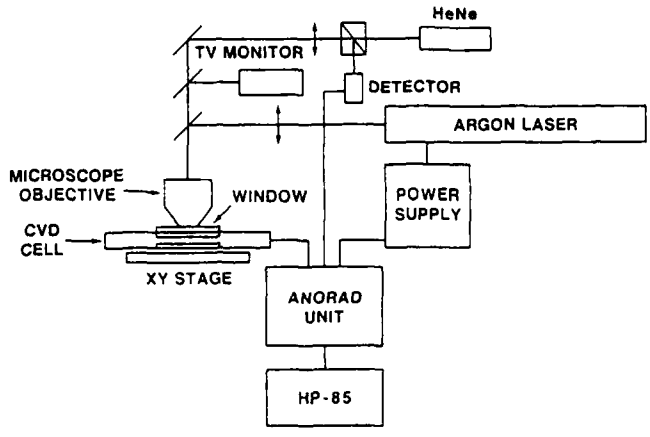

Figure 7. Laser processing apparatus.

A He-Ne laser, operated colinearly with the Argon ion laser for processing, was used for measuring the optical reflectivity and transmission and to provide in-situ process monitoring capability for diagnostics and control. A video camera and monitor were also attached to the process system for direct monitoring and inspection.

4.1.7 Experimental Apparatus The experimental apparatus is shown schematically in Figure 7. An Argon laser (Spectra Physics, Model 171-08) was focussed through a fused quartz window into a chemical vapor deposition reactor containing samples. The focusing lens was an air-spaced, three-element optics with a focal length of 20 to 40 mm. The catalysts were deposited in the power range from 0.005 W to 0.06 W, about half of this power absorbed. The power of the laser was computer-controlled with a power stability better than 5%. The reaction cell was placed on a translational stage with a resolution of 1 μm. The chemical vapor deposition reactor was made of stainless steel and fused quartz window. A silicon vidicon camera was used for process monitoring.

4.2 Laser-Assisted Copper Deposition on Polyimide

To achieve a useful laser metallization process on polyimide, fast scanning rates are required without adverse affects such as surface damage of resultant metal features with poor electrical and mechanical properties. The approach developed in this work was to use a laser to sensitize a polymer surface by introducing a catalytic amount of Pd laser-decomposed from an organometallic palladium compound. This was followed by immersion in an electroless copperplating solution. The process is shown schematically in Figure 8. Since in this process only a few monolayers of Pd atoms are needed to catalyze Cu deposition, we have been able to achieve a much higher laser writing speed, which is an order of magnitude higher than those values previously reported.

The palladium compounds were introduced in the gas phase to the gas cell (as shown in Figure 1) to form an adsorbed layer of organometallic on the surface, or it was applied on the polyimide surface by sublimation or spin-coating from solution. After selective sensitization with laser irradiation, the substrate is immersed in an electroless copper bath. Electroless processes for copper deposition are well developed and are known to produce metal films with good electrical and mechanical properties. Since only a few monolayers of palladium are laser-deposited, carbon contaminants from that process are minimal and therefore good electrical conductivity was obtained.

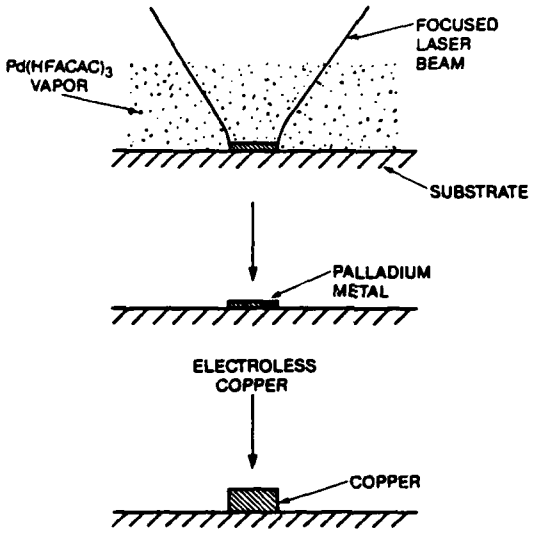

Figure 8. Laser-activated copper deposition process.

4.3 Organometallic Palladium Compounds

Numerous palladium compounds were evaluated as candidate materials for laser deposition experiments. The thermogravimetric analysis (TGA)was used to scan potential materials. The majority of the work was done with three palladium compounds: palladium hexafluoro acetylacetonate (PdHFAcAc), palladium acetylacetonate (PdAcAc), and palladium acetate (PdAc). Each of these compounds has particular physical properties (Table 3) allowing us to evaluate gas phase as well as thin film laser deposition. *In Figure 9 the TGA curves for these three compounds are shown.*

The PdHFAcAc is the most volatile compound and can be easily sublimed on a hot plate. Sublimation starts at 60 °C, and the vapor pressure is extrapolated to be about 1 torr at 75 °C (Ref. 15). The two other derivatives (PdAcAc and PdAc) did not sublime until the thermal decomposition points were reached. At a heating rate of 10 °C/min, PdAc decomposes to palladium metal at 250 °C.

4.3.1 Gas Phase Deposition Gas phase experiments were carried out using PdHFAcAc. Initial experiments were run in a static environment. A few milligrams of the compound were placed in the stainless steel cell (Figure 1) fitted with a quartz window. Two valves were attached to allow evacuation of the cell. The cell was evacuated and heated to the desired temperature prior to irradiation. The gas pressure could be readily adjusted by adjustment of the cell temperature. Results of laser irradiation are shown in Figure 10. After laser irradiation at various power levels, the samples were immersed in an electroless copper solution. At low laser power levels, no palladium deposition (and hence no copper) was observed, which was attributed to the fact that PdHFAcAc is sufficiently volatile to sublime off the surface during laser irradiation. However, local heating caused deformation of polyimide film (Pyralin 2540, Dupont Chemicals) which was spun-on on glass. Deformation was attributed to additional curing of polyimide (imidization,residual solvent loss, crosslinking) due to laser irradiation and was found to be sensitive to the thermal history of curing during sample preparation. The laser power increased to a level which was sufficient to decompose the organometallic compound and caused in palladium deposition and subsequent electroless copper deposits. However, at these power levels, local decomposition of polyimide resulted in a poor morphology of the deposited copper film.

Although fast scan rates of 32 mm/s were achieved, it was difficult to obtain consistent results with this approach. For pyrolytic laser deposition, one would like to have an organometallic compound with a higher vapor pressure for efficient decomposition of the reactant molecules. Partial pressures

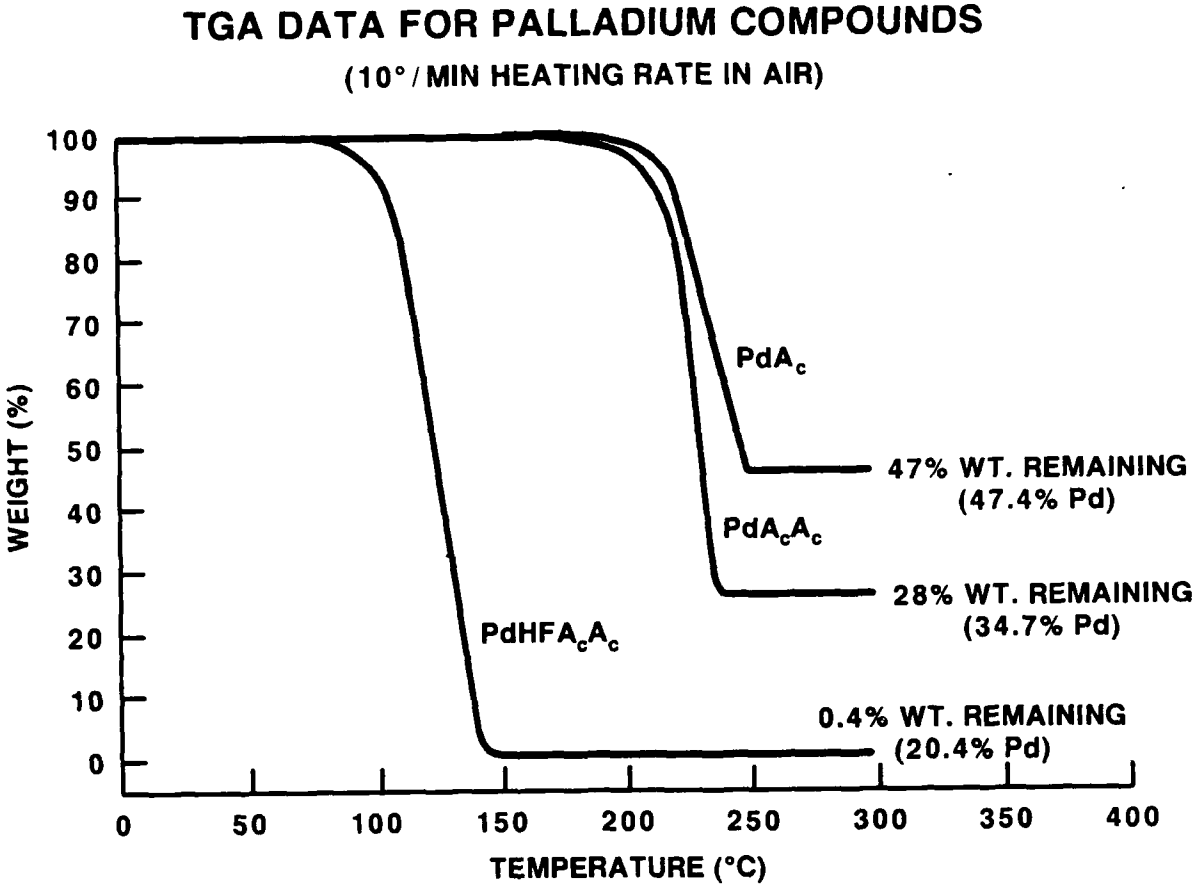

Figure 9. **Thermogravometric analysis data for organometallic palladium compounds studied in this program.**

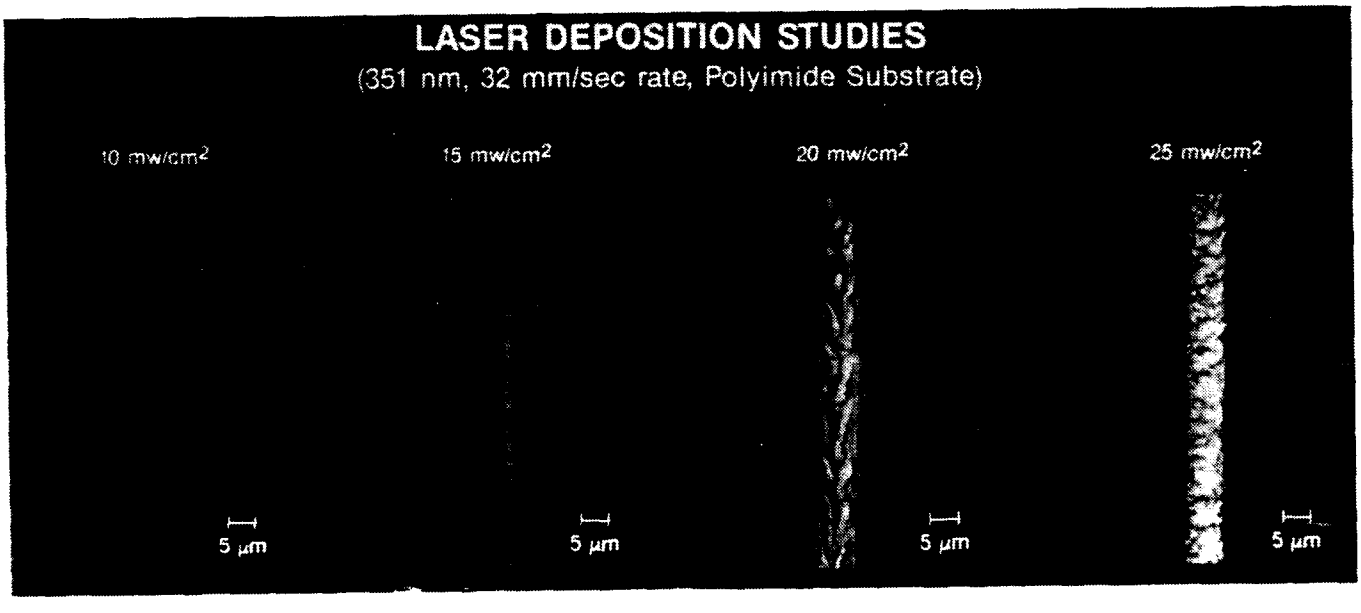

Figure 10. **Laser irradiation of PdHFA$_c$A$_c$ in the gas phase.**

of up to a 100 torr have been obtained for these thermal processes. Ideally, the substrate should be maintained at room temperature or below room temperature such that the adlayers do not desorb from the surface. As the temperature increased, desorption will reduce the adsorbates unless compensated by increasing the partial pressure of the reactant gas. Our gas phase experiments were carried out at temperatures between 60 and 80 °C. At these temperatures, difficulties were encountered due to the fact that the palladium compound sublimed readily and condensed on the gas cell window or on the cell wall. In order to improve our results with gas phase deposition, higher temperatures were required or more volatile palladium compounds had to be identified. Laser deposition experiments at higher temperature were carried out using PdHFAcAc with results which were not satisfactory as described earlier. The compound is not stable at a temperature to have sufficient vapor pressure. At about 100 °C, rapid sublimation of the material caused uncontrolled deposition. To overcome these problems, a flowing CVD system was constructed using argon as the carrier gas purged through a stainless steel bubbler containing PdHFAcAc. The entire system was maintained at 70 °C and the unreacted organometallic was trapped and decomposed downstream from the gas cell. Problems with reproducibility and condensation were still encountered with this organometallic compound.

The experience gained from these experiments led us to conclude that a more volatile Pd compound is required for the gas phase approach to work out successfully. Our emphasis was then placed on the thin film approach to be discussed in detail in the following sections.

4.4 Thin Film Deposition

Several Pd compounds were synthesized during the course of this study including PdAcAc and PdAc. Their properties are summarized in Table 4. These compounds were soluble in a variety of organic solvents and could be conveniently spin coated from solution to produce thin organometallic layers. The thin film process is therefore compatible with the current IC process and offers process advantages being readily transferable to the existing IC technology. After laser irradiation, the samples were rinsed in appropriate solvent to remove organometallic compounds in the unirradiated regions. The samples were then placed in an electroless solution for copper deposition. *Figure 11 shows* the morphology of spin coated films of PdAcAc and PdAc on polyimide surfaces. Although laser deposition was achieved with PdAcAc, the crystalline structure resulted in nonuniform palladium deposition and, hence, irregular copper deposits. Better results were obtained with PdAc because this material produced amorphous films when spun on polyimide surfaces (Refs. 18, 19).

By appropriate control of power and scan speed, smooth uniform copper lines were written in polyimide using thin PdAc films. A plot of power scan speed relationships is shown in Figure 12.

COMPOUND	Pd CONTENT	SUBLIMATION TEMPERATURE (1)	DECOMPOSITION TEMPERATURE (2)	LASER DEPOSITION PROCESS
PALLADIUM (II) - HEXAFLUORO ACETYLACETONATE (Pd HFAc Ac)	20.4%	60°C	200°C	GAS PHASE
PALLADIUM (II) - ACETYLACETONATE (Pd Ac Ac)	34.7%	175°C	220°C	THIN FILM
PALLADIUM (II) - ACETATE (Pd Ac)	47.4%	200°C	220°C	THIN FILM

(1) FROM TGA DATA

(2) FROM DSC DATA

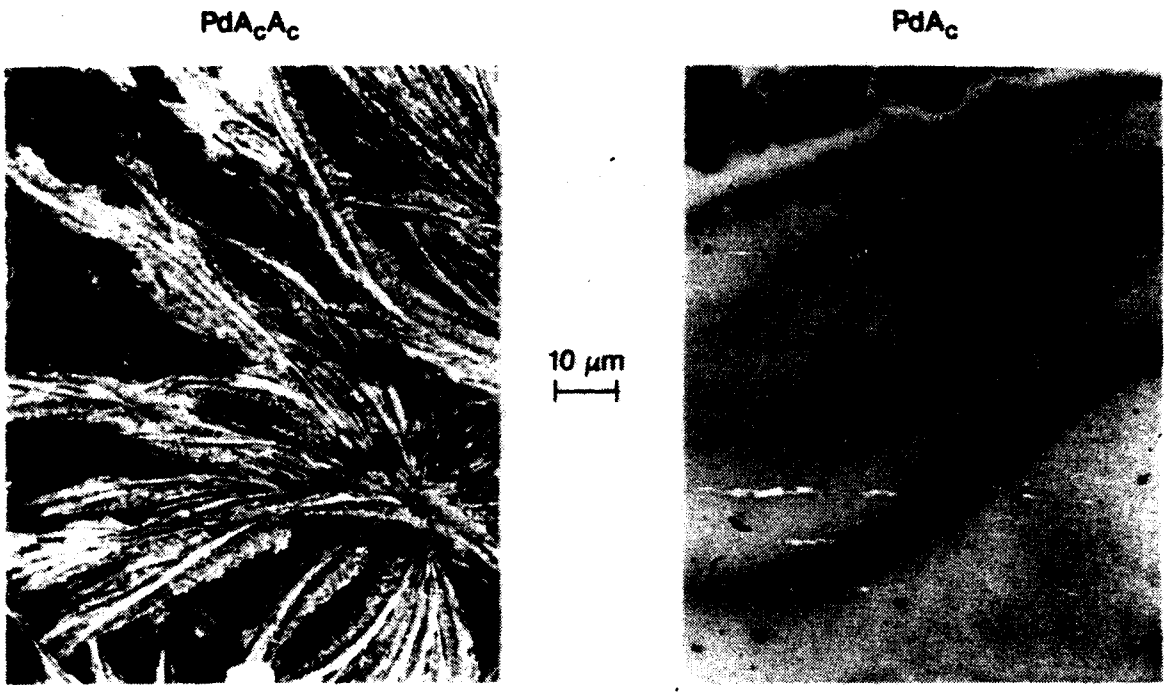

Figure 11. Surface morphology of thin films of PdA_cA_c and PdA_c on polyimide.

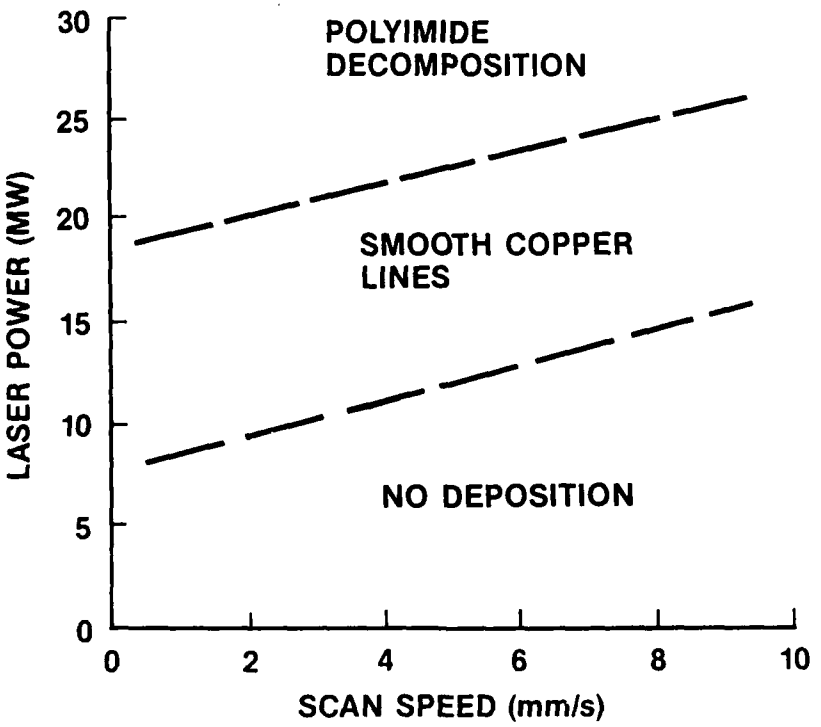

Figure 12. Power/scan speed relationships for laser deposition of PdA_c.

Copper lines up to 1.5-μm thick with resistivities of 3.0 $\mu\Omega$-cm were achieved. The beam diameter used in these experiments was measured to be 28 μm corresponding to fluence levels of 2 to 4 $\times$ 10^5 W/cm^2. As shown schematically in Figure 12, higher power levels caused thermal decomposition of polyimide. At these power and scan conditions, the polymer is ablated off the surface (carrying away Pd and by-products) and resulted in no copper deposition. At lower power levels, pyrolysis of the PdAc is still achieved but the local temperature does not exceed the decomposition temperature of the polyimide film which is greater than 500 °C. In this regime, the laser-activated surface containing palladium lines catalyzes electroless copper deposition with excellent surface morphology.

In this study, we have found that for good quality copper deposition with good adhesive properties, an optimum surface concentration of palladium atoms is critical. The results of this study are further discussed in the following section.

4.4.1 Rutherford Back-Scattering Analysis The Rutherford Back-Scattering spectroscopy was employed to study the surface densities and thickness of palladium deposited on the polymer surface under various thermal- and laser-induced decomposition conditions. The RBS facility, located at the High Energy Acceleratory Laboratory of the Physics Department at the State University of New York at Albany, was recently upgraded to incorporate a microprobe capability with a spatial resolution to about 1 μm under a joint program with GE-CRD (Ref. 20). The microprobe provides a unique capability to spatially resolve Pd distributions of laser-deposited structures with a dimension of 10 to 20 μm. In the following sections, we will describe the RBS facility used in this work, and RBS results for determination of the Pd surface densities, film thickness, and spatially resolved Pd distributions under various thermal- and laser-processing conditions. These results are compared with those of electroless deposited copper to determine the optimum Pd sensitization condition for the electroless copper deposition. We have found this is a most critical parameter for achieving a good copper deposition using the electroless deposition technique.

4.4.1.1 RBS and MicroProbe Facility The facility is equipped with a microprobe beam and the experiments conducted here employed both RBS and microprobe analyses. The 2 MeV He^+ beam leaves the accelerator analyzing magnet with a divergence of about 1 mrad. The beam drifts a distance of about 275 cm to a quadruple lens and is focused on the microslit after another 320 cm drift path. Electrostatic steering plates were placed after the first quad lens to control the focused beam position.

The beam current exiting from the accelerator analyzing magnet is typically 1 to 10 μ-A of He^+ ions at 2 MeV. With the final autoalign control slits defining an aperture 200 $\times$ 200 μm, about 0.1 μ-A will pass on to the microslits. For a smaller aperture, the beam current will reduce accordingly. For 1 to 2 μm size beam, the beam current is estimated to be 200 to 400 pA at the specimen.

The target alignment was achieved using the secondary electron image formed by scanning an 1.5 MeV proton beam impinged upon the sample. A simple aluminized plastic scintillator is biased at +10 kV to accelerate, attract, and convert the low energy secondary electrons to light pulses. These are then converted into an electrical current in a photomultiplier, and constitute the video signal for reconstructing the image. The X-Y positioning is controlled by a personal computer that is also used to control and read RBS data from the multichannel analyzer.

4.4.1.2 RBS Results

4.4.1.2.1 Surface Pd Concentration and Effects on Copper Deposition The quality of copper deposited from electroless copper deposition was observed to depend critically upon the surface concentration of Pd used as the catalyzing agent. In order to determine the optimum Pd surface concentration the following RBS experiments were carried out.

Chloroform solutions containing various amount of PdAc were prepared and spin-coated at 2,500 rpm for 30 s on the polyimide substrate to deposit a thin layer of amorphous PdAc film of about 2,500 Å

thick. The samples were then baked at 250 °C for 15 min, followed by dip and rinse in chloroform. A set of samples was used for RBS analyses to determine the Pd surface density as a function of the initial PdAc concentration in the chloroform solution. Figure 13 shows the RBS spectra for samples prepared with initial 0.1%, 0.2%, 0.5% and 1.0% (by weight) of PdAc in chloroform. The spectra were calibrated against a Cs sample to determine the absolute Pd surface concentration.

The Pd surface densities were determined to be 3.2, 5.4, 16.4, and 23.3 x 10^{15} atom/cm^2 for 0.1%, 0.2%, 0.5%, and 1.0% samples, respectively, and were found to vary almost linearly to the initial PdAc concentration dissolved in chloroform.

Another set of samples prepared using the identical procedure were placed in the Shipley 406 electroless copper bath solution for 10 min. The samples after copper deposition were examined first visually, then subjected to scotch-tape tests. The quality of copper deposited was found to depend critically upon the Pd surface concentration, and the optimum Pd concentration was determined to be in the range of 3 to 5 x 10^{15} Pd atom/cm^2 corresponding to a few monolayers of Pd on surfaces. After the optimum Pd surface concentrations of thermally decomposed PdAc samples were determined, 1% PdAc dissolved in chloroform and span on polyimide were used as the standard in the subsequent experiments.

Surface concentrations of laser-deposited Pd on polyimide were also analyzed using RBS. An argon laser at 351 nm was focused to a spot of about 28 μm in the power range between 3 mW to 30 mW.

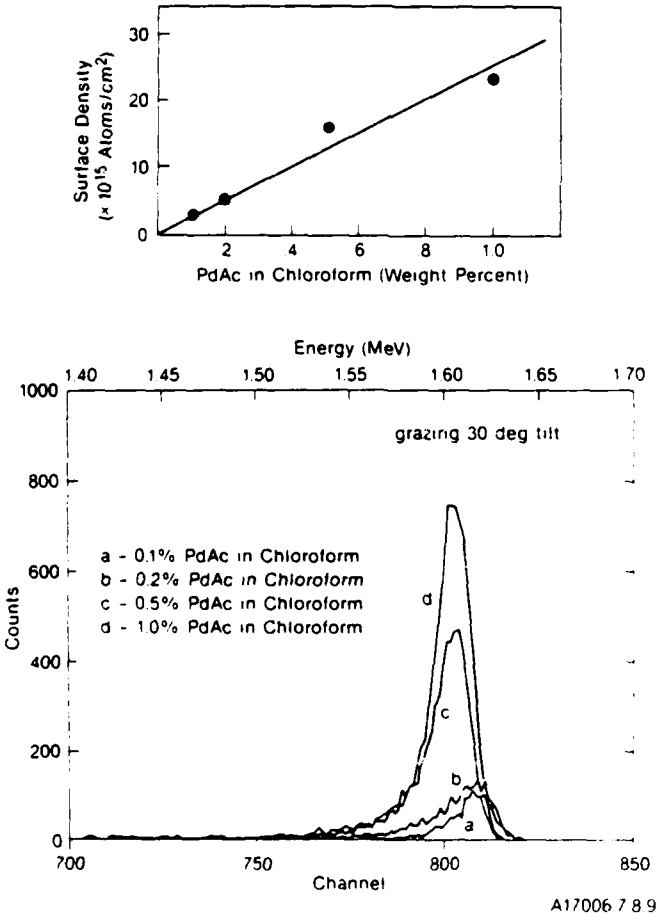

Figure 13. RBS spectra and surface densities of thermally decomposed Pd on polyimide (effect of concentration).

Multiple laser scans were used to produce an exposed area of 5 mm by 5 mm with a scanning speed varying from 0.5 cm/s to about 5 cm/s. Figure 14 shows the Pd surface concentrations measured as a function of 1/power.

Since the surface temperature induced by laser radiation is linearly proportional to the irradiation power, the log plot of Pd surface concentration as a function of $1/T$ is a straight line with the slop proportional to the activation energy of thermal decomposition reaction of PdAc. This will be further discussed in the section on "Laser-induced Reaction Kinetics." Figure 15 shows the Pd surface concentration measured as a function of the normalized dwell time, $1/V$, where V is the scan speed.

As shown in the figure, the Pd surface concentration for laser irradiated polyimide, spin-coated with 1% PdAc dissolved in chloroform, increases from 1.1×10^{16} Pd atom/cm^2 at 1 ms normalized dwell time (relative) to about 2×10^{16} Pd atom/cm^2 at 8-ms normalized dwell time. At slower scanning speeds, i.e., longer dwell time, the Pd surface concentration saturates at a value of about 2.2×10^{16} atom/cm^2. Saturation of the Pd surface concentration as a function of laser dwell time indicated a completion of Pd thermal decomposition from PdAc within a dwell time of about 5 ms at 20 mW laser power. The saturation of Pd surface concentration also explained the relative insensitivity of copper line width observed as a function of the laser scanning speed.

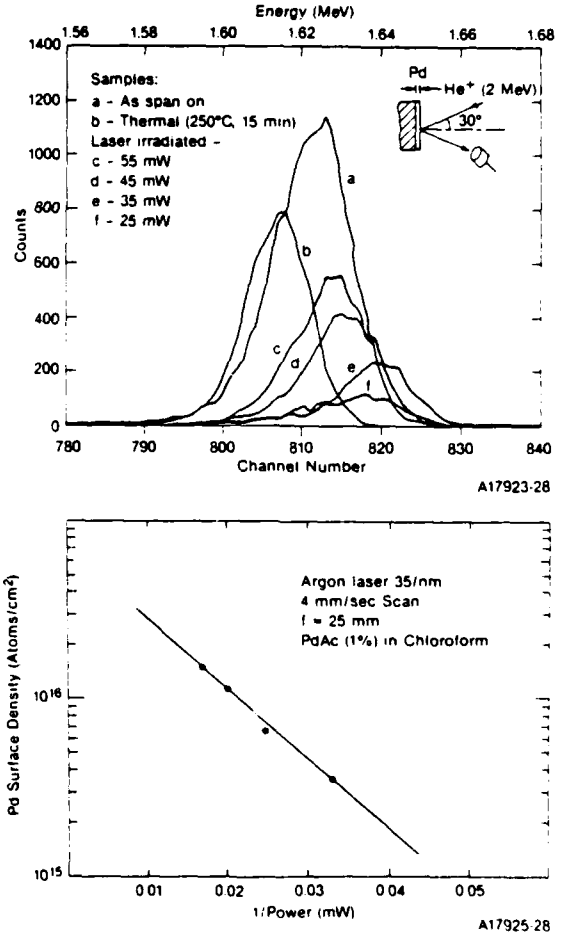

Figure 14. RBS spectra and surface densities of laser-activated Pd on polyimide (effect of power).

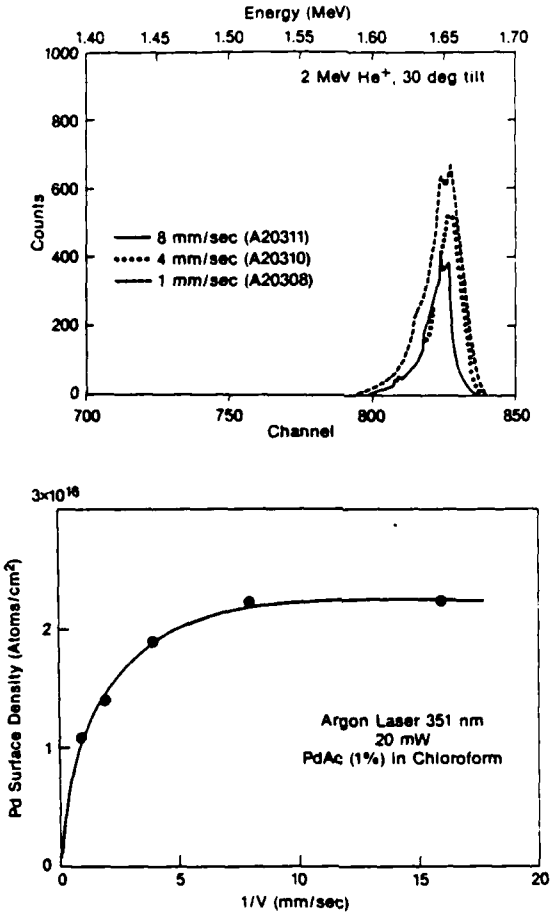

Figure 15. RBS spectra and surface densities of laser-activated PD on polyimide (effect of scan speed).

4.4.1.2.2 3-D Pd Distribution Analyzed with RBS Imaging The RBS microprobe can be operated in the image mode in which a Synertek SYM-1 microcomputer equipped with 3-bit planes of video memory to give a 320 H by 200 V by 8 grey level image that can be displayed in a continuous manner on a TV monitor. The SYM-1 contains digital to analog converters, which generate the scan waveforms. The image was formed by collecting the secondary electrons emitted as the 2 Mev He^+ ions was scanned in 320 H by 200 V raster. Typical beam current was about 0.3 nA and the frame recording time was 5 s. The beam size was estimated to be about 1 to 2 μm. The digital image was transferred to a 24 kbyte file on a floppy disk, then subsequently read into a Zeiss IBA image analyzer system from which photographic prints were made. Figure 16 shows a result of RBS image of laser activated Pd on polyimide surfaces. Figure 16a shows a printout of the Pd image on a 200 x 200 μm scan; the dark stripes are areas laser-scanned at a speed of 2 mm/s at 20 mW. The sample was rinsed in chloroform after the laser exposure to remove residue PdAc in the unexposed areas. Figure 16b shows a three-dimensional Pd distribution on the sample area displayed in Figure 16a. The peak Pd distribution at the line center was about 4×10^{15} atom/cm^2 with decreasing Pd surface concentrations on both sides of the laser scan lines separated by 100 μm spacing. Since the surface Pd concentration induced by laser radiation is only about 1 to 2 monolayers, the RBS imaging technique proved to be a sensitive technique for analyzing surface distribution of catalysts such as Pd on a polymer surface.

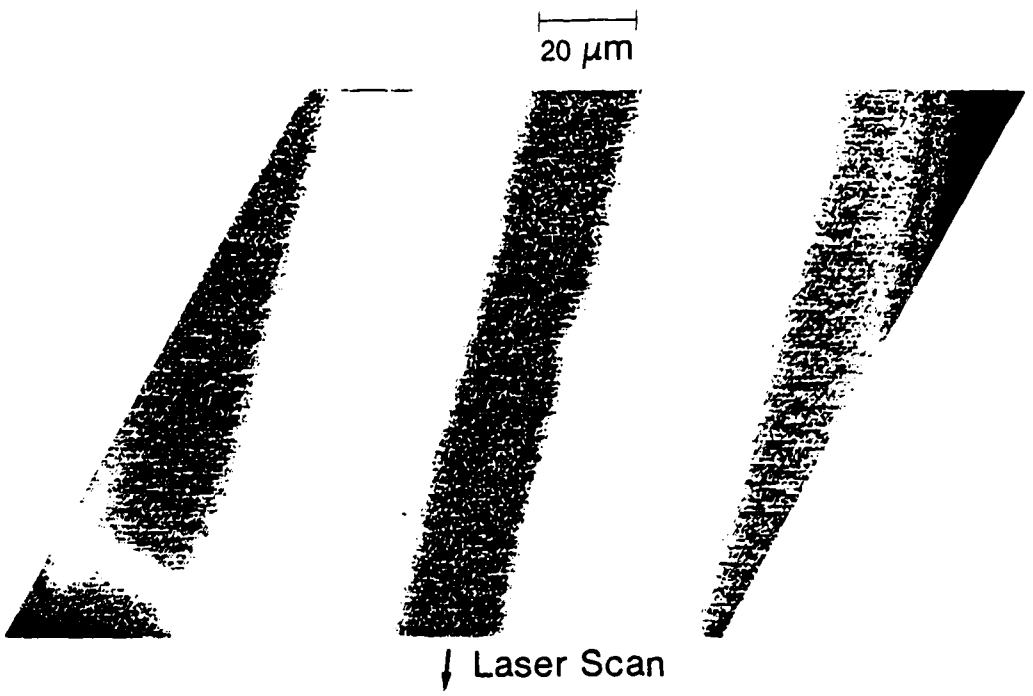

(a) Image of Pd Atoms

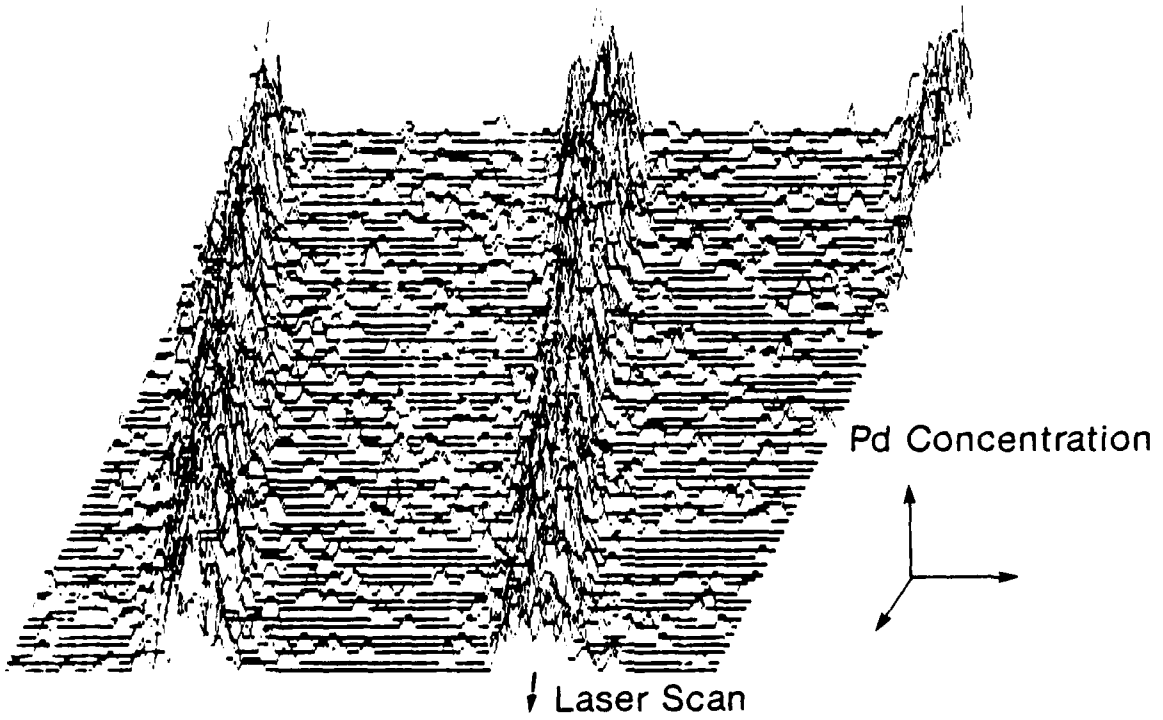

(b) Pd Surface Distribution in 3D Representation

Figure 16. RBS microbeam secondary electron image of Pd distribution.

4.4.2 Electroless Copper Deposition The electroless copper deposition process was chosen for the present study because it produces copper with excellent electrical and mechanical properties, and is widely used in the electronic industry for circuit board and electronic packaging applications. (For a review of these techniques, see Refs. 21 and 22.) The process was first applied to plastics in the early 1960s when it was found that etched surfaces of ABS polymers enabled some adhesion to occur such that a plated metal could be bonded to the polymer surface. Group VIII elements of the periodic table have been shown to provide the necessary catalytic effect to initiate deposition. The process involves pretreating the polymeric surface with catalyst, for example by immersing in a dilute solution of a tin or palladium compound or solution. The sample is then placed in the electroless bath which is formulated to be more electronegative than the catalyzed surface. A replacement reaction occurs that is self-perpetuating because the deposited metal is itself a catalyst for the reaction. The chemistry of the bath is critical for such characteristics as speed of deposition, brightness of deposit, and thickness of metal deposited.

Commercially available baths are available although the chemistries involved are guarded. For our purposes, commercially available electroless copper baths were first evaluated to determine which process yielded the best deposits. We were concerned with the absolute thickness obtainable as well as the electrical and mechanical properties. The baths evaluated are shown in Table 5.

Table 5

EVALUATION OF ELECTROLESS COPPER PLATING BATHS

Electroless Copper Bath	Manufacturer	Plating Rate	Maximum Thickness	Resistivity
Cu-402	Enthone Corp.	300 Å/min	0.4 μm	6.0 μΩ-cm
Cu-406	"	300 Å/min	0.3 μm	6.0 μΩ-cm
Cu-872	"	300 Å/min	0.3 μm	--
Cu-328Q	Shipley Co.	300 Å/min	0.3 μm	--
Cu-250	"	300 Å/min	1.5 μm	3.0 μΩ-cm
Cu-9620	McDermid Co.	200 Å/min	5.0 μm	11.0 μΩ-cm

In these experiments, palladium acetate was spin coated from solution on polyimide substrates and was baked for 15 min at 225 °C prior to immersion in the plating bath. Thickness measurements were made using a surface profilometer and resistivities were measured using a standard 4-point probe method. Immersion times of 10 to 15 min were possible with thickness build to about 0.4 μm. Longer immersion times usually resulted in peeling or cracking of the copper layer. The MacDermid bath and Shipley 250 were able to coat thicker layers without cracking or peeling. Of these two, the Shipley bath gave more reproducible results and also resulted in better quality layers as evidenced by the lower resistivity values. Copper layers produced from the shipley bath were found to have good adhesion. Standard peel strengths of 6 lb/in. were recorded.

4.4.3 Laser-Induced Reaction Kinetics The thin film process is schematically illustrated in Figure 17 including micrograph inserts showing the processed samples at the end of each process step. The discussion presented here describes only the thin film approach which is the most attractive method for sensitizing a polymer surface using low vapor pressure organometallic compounds.

Laser-Activated Cu Deposition on Polyimide

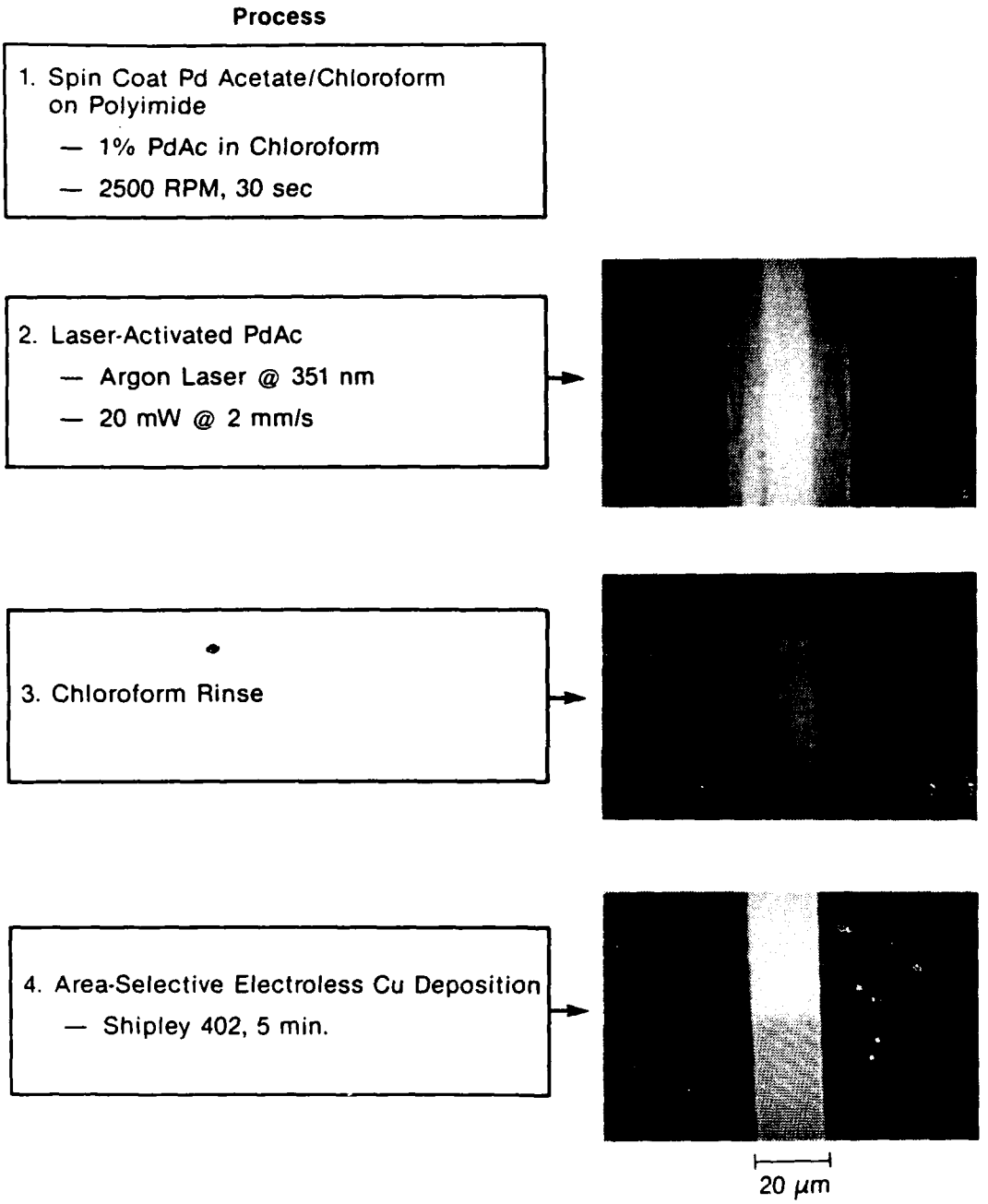

Figure 17. Thin film process for laser-activated metal deposition.

As shown in Figure 17, the process steps include

1. spin coat chloroform solution containing 1% PdAc (by weight) on polyimide (Kapton) at 2,500 rpm for 30 s,
2. exposing the sample to a focused Argon laser beam (351 nm) at a power level 5 to 30 mW and scanned at speeds of 1 to 20 mm/s,

3. after the exposure, rinsing the sample in chloroform to remove the residues in the unexposed area containing organometallic precusors, and
4. placing the sample in an electroless plating solution (Shipley 402 for 5 min at room temperature) to selective deposit copper.

Before laser exposure, the PdAc thin film spin-coated on polyimide was examined closely under a high magnification microscope and was found to exhibit an amorphous structure. This is a key requirement in producing uniform and smooth metal lines. After laser exposure, the exposed area showed a visible track. Depending upon the laser power and scan speed, the apparent width and surface morphology varied. After the chloroform rinse, the changes of surface morphology became much less pronounced, and under some exposure conditions, these were almost no visible effects observed. The final copper deposition depended strongly on the laser power, and to a lesser extent on scan speed. Excellent copper deposition was achieved at a laser power of about 20 mW and at scan speeds of 0.5 to 2 mm/s as shown in Figure 18.

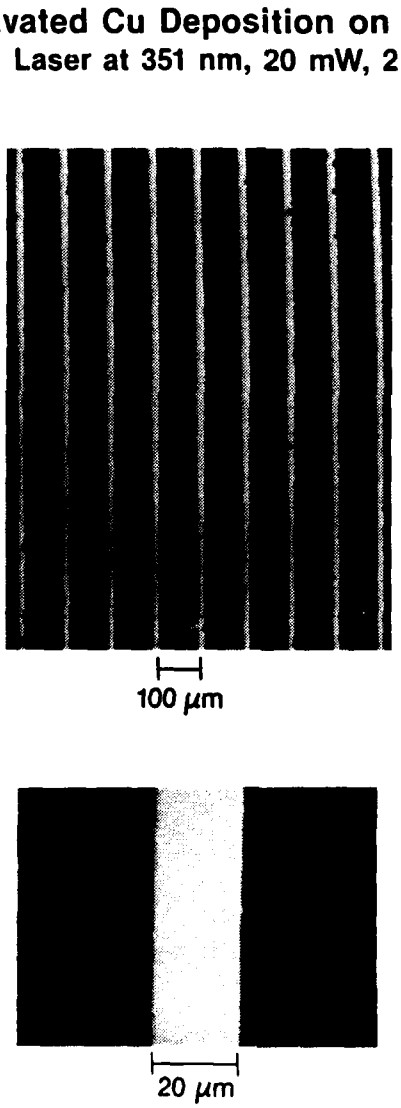

Figure 18. Laser-activated Cu deposition on polyimide (from PdA_c).

Figures 19 and 20 show a series of micrographs taken at various stages of process steps to depict the results of laser exposure, chloroform rinse and selective copper deposition using the process developed. The photos in Figure 19 were taken under two different laser power conditions, e.g., 20 mW and 30 mW at a constant scan speed of 2 mm/s. Higher laser power produced a wider line width until the power reached to a level at which the substrate damage occurred. At a power level of 30 mW and

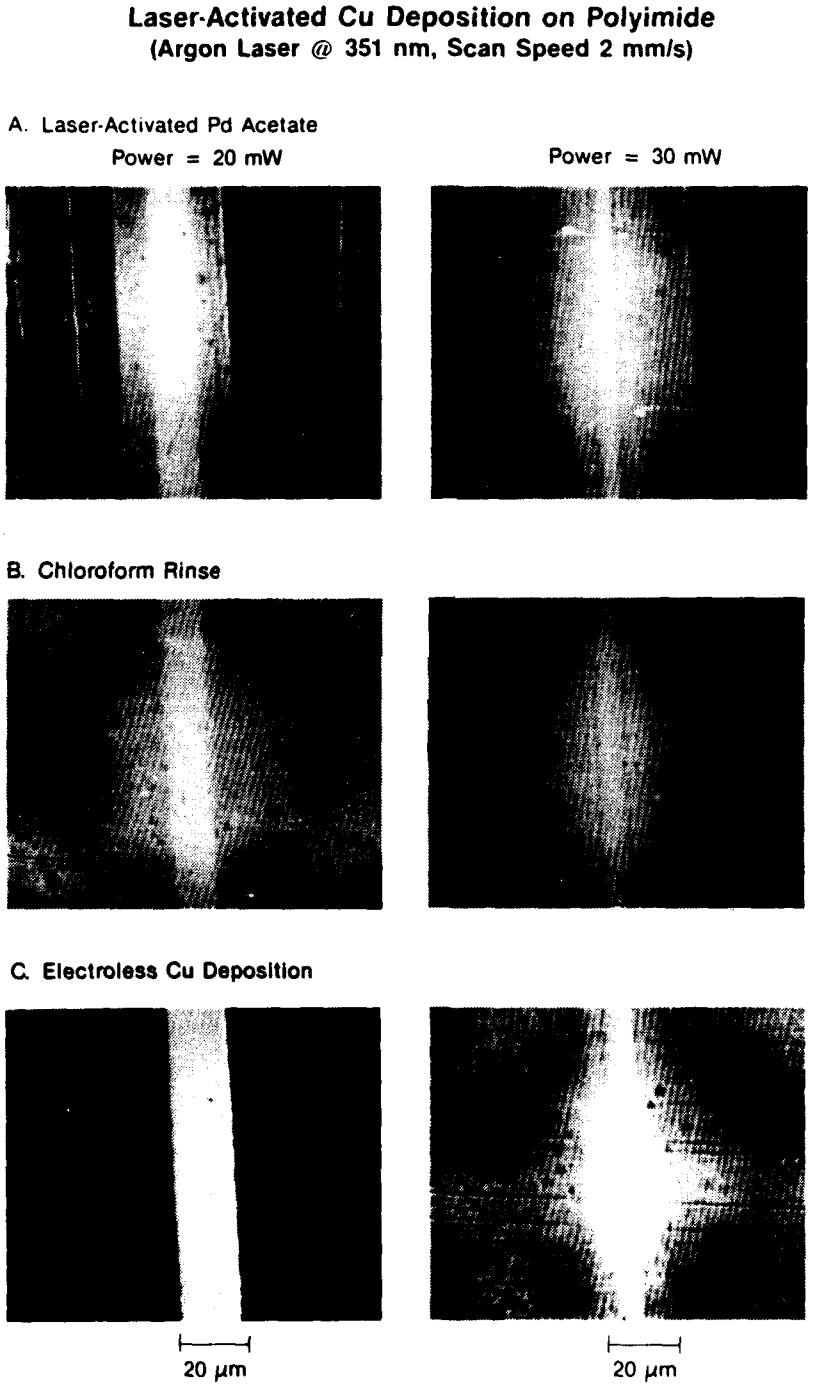

Figure 19. Photomicrographs of laser processing sequences at constant scan speed for 20 mw and 30 mw power levels.

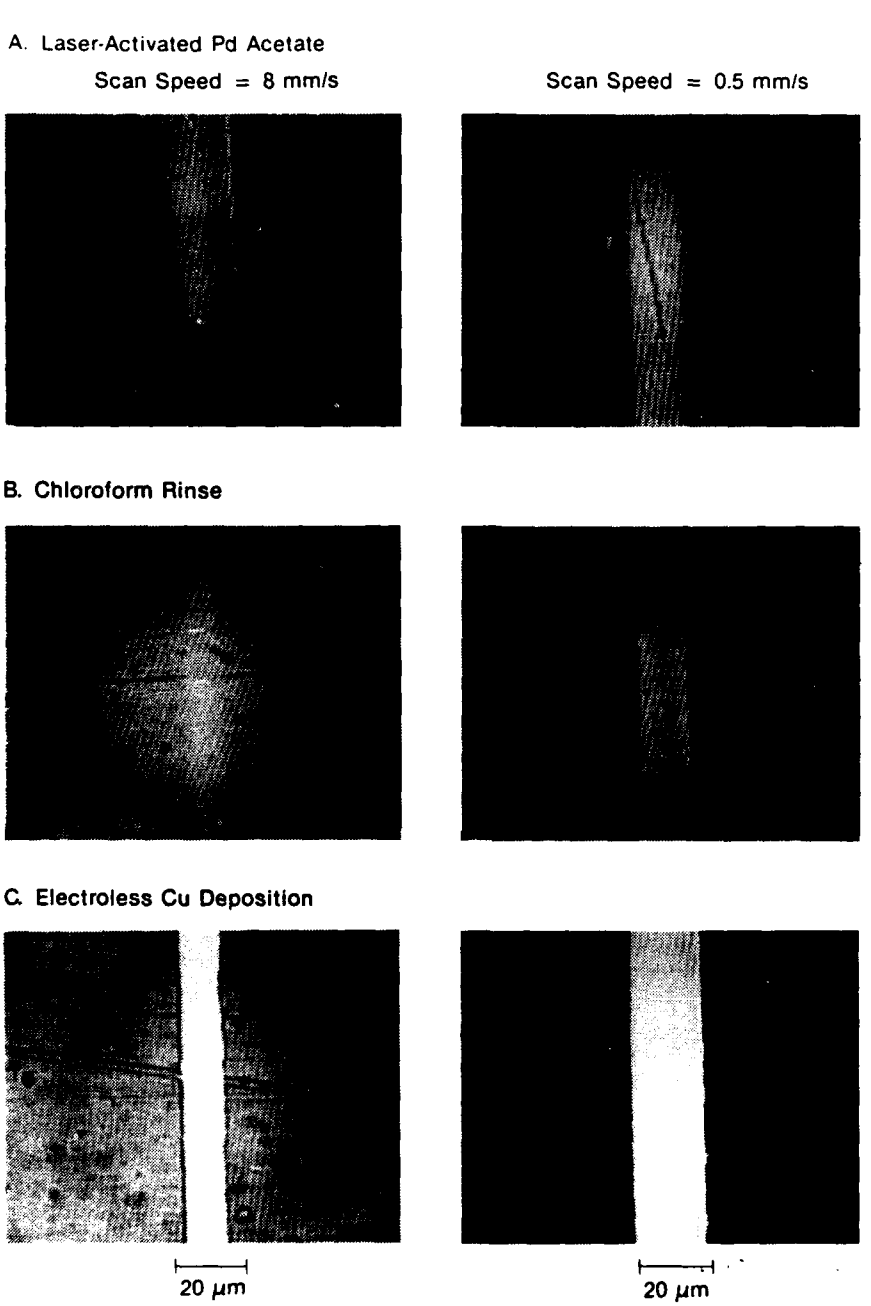

Figure 20. Photomicrographs of laser processing sequences at constant power for 8 mm/s and 0.5 mm/s scan speeds.

at the scan speed of 0.5 mm/s, severe damage tracks were observed on the polyimide surface. At the same power level (30 mW), the apparent damage became significantly reduced by increasing the scan speed to 2 mm/s. At this power level, however, after rinse and electroless plating, no copper deposition was observed. Reducing the laser power to 20 mW at 2 mm/s, copper lines with smooth surface morphology were produced. At 20 mW power level, excellent copper deposition was achieved over a relatively wide scan speed range varying from 0.5 to 8 mm/s.

To further investigate the laser-induced reaction kinetics in the current copper deposition process, we chose the following set of parameters:

w = apparent line width measured from micrograph (μm)
P = laser power (mW)
$1/P$ = inverse of laser power
V = scan speed (cm/s)
$1/V$ = normalized dwell time

The apparent linewidths measured as a function of laser power with a microscope after laser scans, chloroform rinse, and electroless deposition are summarized in Figures 21a, b, and c. Figure 21a shows the initial structures observed after the laser scan. The line width increased linearly proportioned to the incident laser power. After sample rinse in chloroform, the line structures were less visible except for high power (>25 mW) when the substrate damage occurred. In addition, the rinse generally reduced the apparent line widths by about 50%. After electroless deposition, the copper line width was observed to increase as a function of laser power to about 20 mW, and then the copper line width started to decrease. There were no copper deposition when the laser power reached about or over 25 mW. (Figure 21c). At this power level, the damage of the polyimide surface occurred resulting in a surface that has very poor adhesion. The substrate surface damage thus places an upper limit for the power level operable. At 351 nm argon laser wavelength scanned over a Kapton surface, we found this maximum power is about 30 mW at a spot size about 30 μm and at a scanning speed of about 1 mm/s.

Figure 22 shows the line width measurements plotted as a function of $1/V$, defined as the normalized dwell time of the laser scan. The line widths after the laser scan are shown in Figure 22a. The width increased initially as a function of dwell time, then quickly saturated at a normalized dwell time above 0.5. At a constant power, the laser-written line width is controlled by the following parameters – the dwell time, thermal diffusion time and the degree of consumption of the precusors deposited on the polymer surface.

From an earlier RBS measurement, we had determined that PdAc was completely decomposed at a scan speed of 2 mm/s at 20 mW, and with 1% PaAc dissolved in chloroform spun-on polyimide. This resulted a complete consumption of Pd precusors. Compared with the results shown in Figure 22, saturation of the Pd line width started to occur at about the same scan speed of 2 mm/s. This property is unique with the current thin film approach where the supply of the reactants is fixed. Similar behaviors of the line width variation as a function of the dwell time were also observed for samples after rinse and after electroless copper deposition. In both of these cases, however, line widths were reduced from the values measured after the laser exposure.

These results suggest that the following reaction kinetics and thermal characteristics are critical for the laser activated metal deposition process studied here.

(a) Power: The maximum laser power is limited by the local temperature at which the surface decomposition of polyimide occurs. From our study, we put the maximum temperature at about 600 °C and the laser power at about 25 mW at 351 nm. Below the maximum laser power, the temperature increased linearly as a function of the laser power. This is to be compared with a calculation of the polyimide surface temperature induced by the laser irradiation as a function of the laser power for various scan speeds, as shown in Figure 23. A minimum power is required to raise the surface temperature high enough to thermally decompose Pd precusors. From a TGA analysis, this temperature was determined at about 250 to 280 °C. From the calculation, at a scan speed of 2 mm/s, the laser power required to reach this decomposition temperature is about 7.5 mW. This is in good agreement with the copper line width measurements as a function of the laser power that showed that a minimum power of above 8.3 mW was required in order to deposit copper in the electroless process.

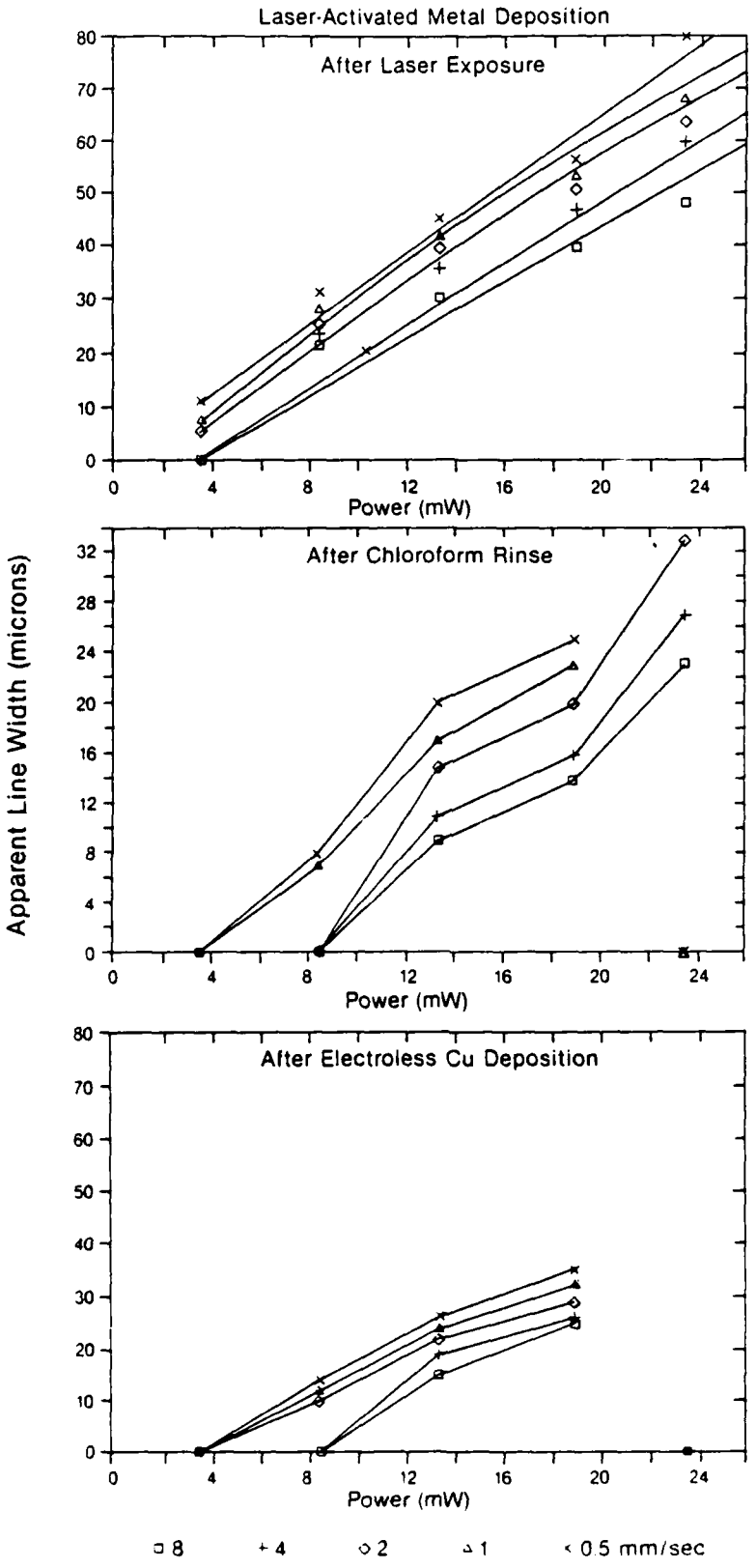

Figure 21. **Effect of apparent line width at various process steps as a function of laser power.**

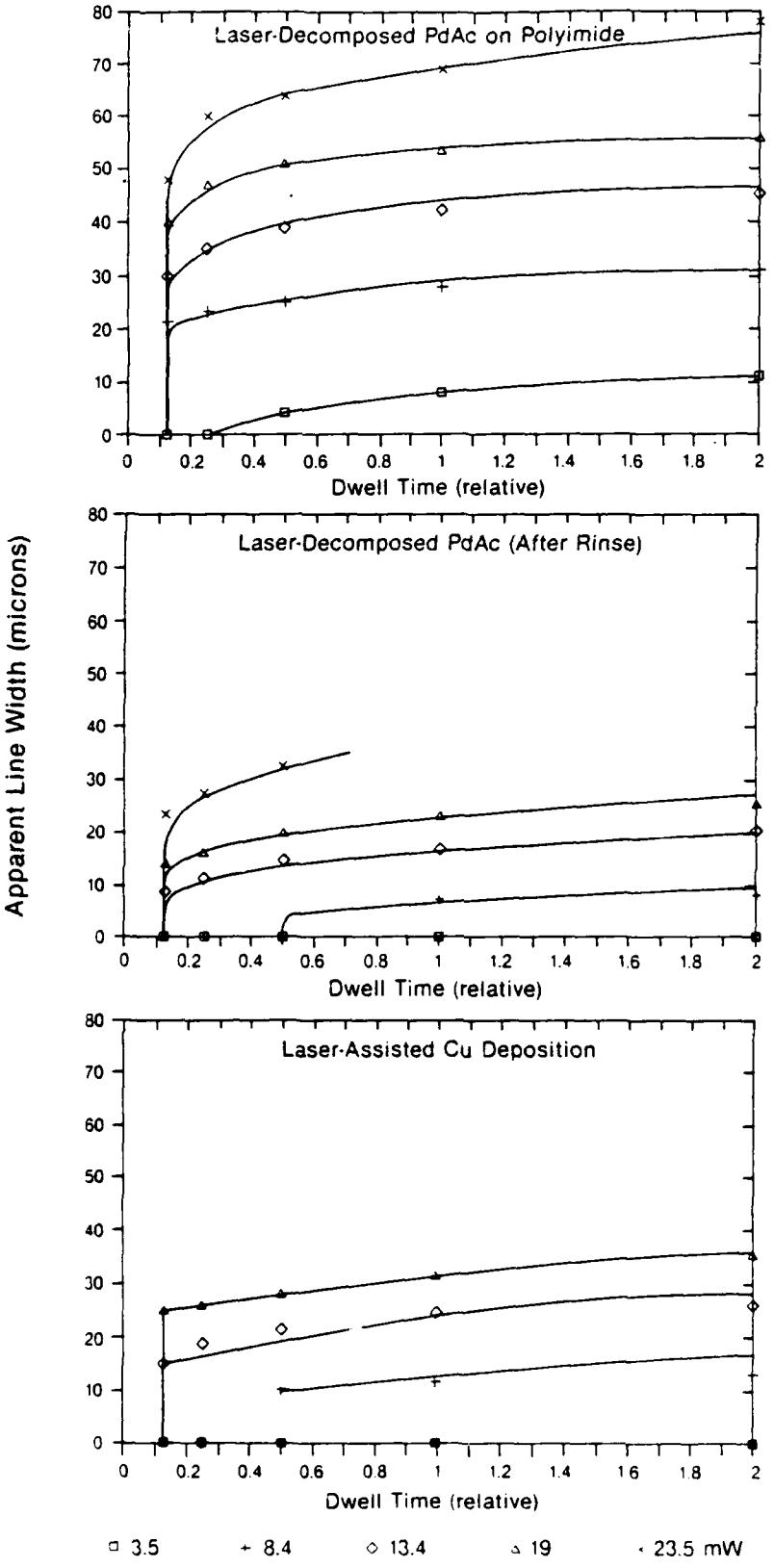

Figure 22. **Effect of apparent line width at various process steps as a function of normalized dwell time.**

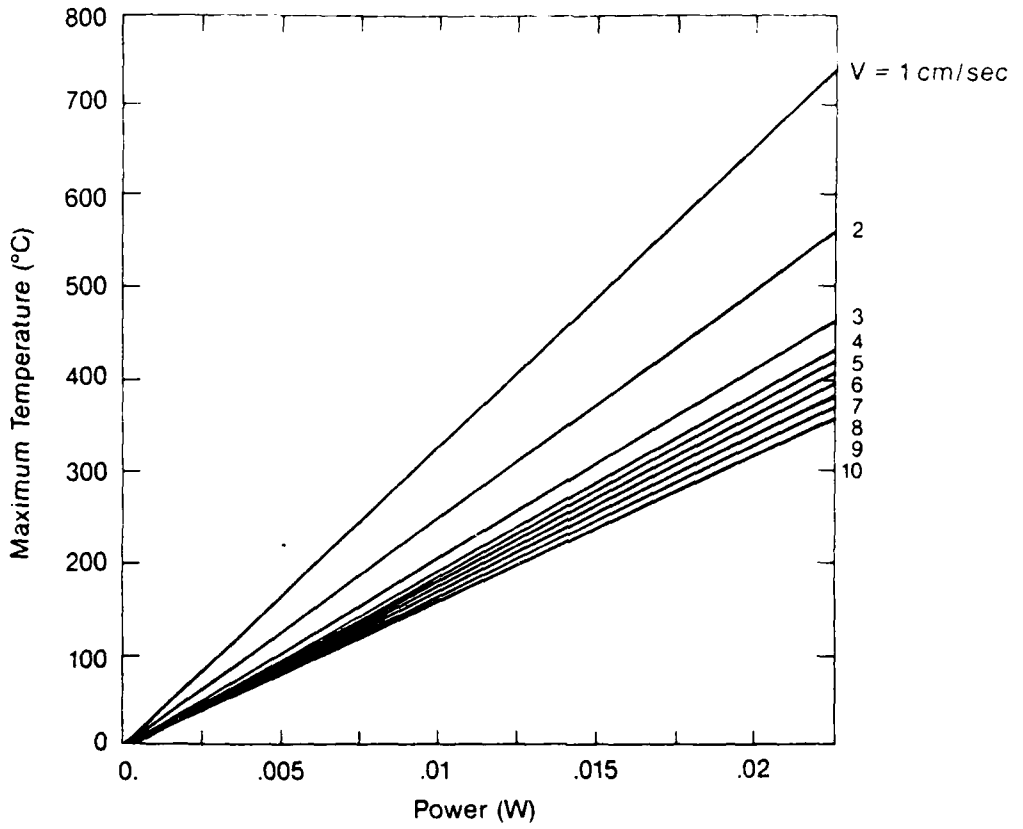

Figure 23. Maximum polyimide surface temperature vs. laser power for various scan speeds.

(b) Spot size: Spot size is a critical parameter that affects the process condition. The minimum spot size that can be focused is equal to the product of the focal length and the beam divergence. In the present study, a focusing lens with a focal length of 40 mm was typically used. With a laser beam divergence of 0.6 mrad at 351 nm, the spot size has a theoretical value of 23 μm. We measured the focused spot size using a knife-edge technique. The laser was focused and scanned over a sharp edge of an aluminum stripe deposited on a glass plate. The reflectance from the focused laser beam was measured with a photodiode. The spot size thus determined was 28 μm (e^{-1} point) when focusing with a 40 mm focal length lens. The discrepancy between the measured value and the theoretical value was due to the aperture used in our experiments that could have increased the beam divergence larger than the specified value of 0.6 mrad.

(c) Scan speed: the scan speed determines the effective dwell time during the laser exposure which is equal to D/V, where D is the beam diameter and V is the scan speed. For a beam spot size of 28 μm, the dwell time is 2.8 ms at a scan speed of 1 cm/s. In our analysis throughout this study, a normalized dwell time, $1/V$, was used for simplicity. The dwell time affects both the temperature and thus the reaction rate at a given laser power. Figure 24 shows a calculated maximum temperature of a polyimide surface plotted as a function of the normalized dwell time, $1/V$, at various laser power levels. At small dwell time (i.e., fast scan), the maximum temperature increases as the dwell time increases until the value of dwell time becomes comparable to the thermal diffusion time of the substrate material. Beyond this value, the temperature increases slowly as a function of the dwell time. If we assume the rate of thermal decomposition follows an Arrhenius-type rate with an activation energy of E_a, then it can be shown that the rate of thermal decomposition increases at a faster rate as a function of the dwell time.

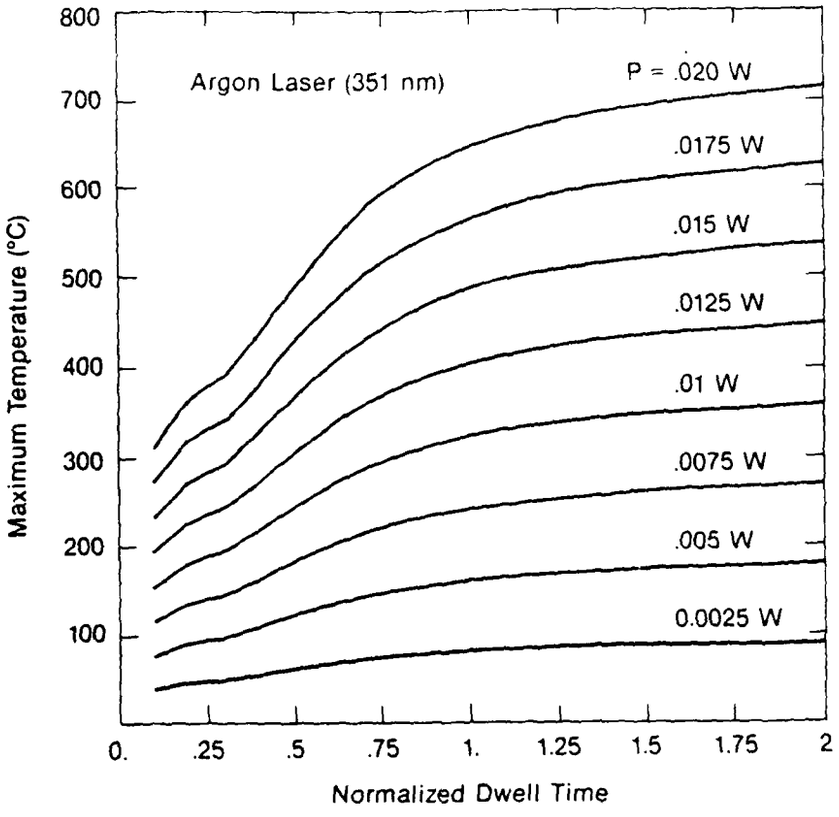

Figure 24. Maximum polyimide surface temperature vs. normalized dwell time.

Section 5

SUMMARY OF KEY TECHNICAL RESULTS

A survey of laser-driven processes for metal deposition from organometallic compounds was completed and promising organometallic compounds were synthesized and evaluated during this study. Various thin film deposition processes were investigated and a laser-activated metal deposition process providing a fast writing speed was developed.

The process is to selectively deposit copper on polyimide using laser irradiation of organometallic palladium compounds. A CW argon ion laser at 351 nm was used to introduce catalytic amounts of palladium prior to electroless Cu deposition. Subsequent immersion of the irradiated samples in an electroless copper solution resulted in copper deposition. Since only a few monolayers of palladium were needed to catalyze the electroless copper process, fast writing speeds of up to 10 cm/s were demonstrated. Copper lines with 1.5 μm thickness and line width of 7 μm to 50 μm and resistivities of 3.0 $\mu\Omega$-cm were produced by this technique. Thin layers of PdAc spin coated on polyimide were shown to produce high-quality copper lines. By using the RBS analysis, the optimum surface concentration was determined to be about 4×10^{15} Pd atoms/cm^2 for copper deposits with good mechanical and electrical properties. This value could be controlled by adjusting the PdAc concentration in the solution. Laser-induced thermal reaction kinetics were also discussed and key processing parameters were identified.

Section 6

KEY TECHNICAL ISSUES

Three key issues were identified for future studies in order to implement this process for high-speed interconnect technology: (1) adhesion of Cu/polyimide system, (2) electrical characterization, and (3) thermal conductivity mismatch.

6.1 Adhesion of Cu/Polyimide System

In general, sputtered or evaporated copper does not adhere well to polyimide. It has been shown that metal/polymer adhesion can be improved by two mechanisms: mechanical or chemical. Metals such as titanium and chromium have been shown to form chemical bonds with polyimides, but there is little evidence for this bonding in copper/ polyimide interfaces. Since the polyimide surface is smooth, it is not unexpected that poor adhesion results. In our laser-irradiated polyimide samples, peel strength measurements were surprisingly high. A value of 6 lb per inch was measured on laser-irradiated films. Copper has been shown to have good adhesion to carboxylic acid groups, and this might account for the good adhesion numbers we have observed. If during laser irradiation we have sufficient energy to thermally decompose or dissociate the imide structure on the polymeric surface, the resultant could be conversion to the amide-carboxylic acid structure.

Additional studies are needed to determine the conditions under which adhesion is optimized and to evaluate the role of laser irradiation. We have also observed a loss in adhesion on thermal aging. This phenomenon and the role of intermediate layers to improve adhesion in the copper/polyimide structure need further investigation.

6.2 Electrical Characteristics

For high-density interconnects, high conductivity is required. We have achieved resistivity values of 3 $\mu\Omega$-cm on laser-irradiated samples subsequently electroless copper plated. We are currently able to deposit copper layers about 1.5 μm thick. Additional work is needed to optimize the electroless plating thickness to achieve 3.0-μm thick copper with low resistivity.

6.3 Thermal Conductivity Mismatch

Since the process employed in the present study is a thermal process, changes in the thermal properties of the substrate surface are going to affect the laser deposition condition and make it difficult to apply the process to surfaces of different characteristics. For example, in the actual interconnect application, contacts have to be made to the aluminum pads. The thermal conductivity of aluminum is several orders of magnitude higher than that of the polyimide. Under similar conditions of argon laser deposition on polyimide, we have not observed deposition of palladium on aluminum. However at 266 nm, using a frequency-quadrupled YAG laser, we have been able to photochemically decompose PdAc on polyimide as well as on aluminum. The writing speeds are high, and this appears to be a promising approach for solving the thermal mismatch problem by using the photochemical process.

Section 7

PROGRAM RECOMMENDATIONS

In view of the potential application of the laser-activated metallization process for high-density, high-speed interconnection technology, we have proposed to the U.S. Office of Naval Research a continuation of this effort in a GE Quotation CRD 5120.019C entitled "Laser Processing for Interconnect Technology," August 1987. As outlined in that proposal, the objective is to develop and investigate fundamental materials and processes necessary for developing this advanced interconnect technology, which is a major ongoing development program at GE-CRD. The program is divided into three basic tasks as outlined below.

1. Continuing our current effort under Contract No. N00014-85C-8090, we propose to further study the laser-assisted metal deposition approach for interconnect metallization. Direct-write metal deposition from organometallic compounds has potential utility for interconnect applications and for yield enhancements. We have demonstrated a laser-activated copper deposition approach. Studies of adhesion to underlying metals and to polymer substrates, contact resistance, conductivity, writing speed, and reliability require additional effort and are proposed in this program for interconnect metallization.
2. *Studies of via hole formation:* Two approaches for laser drilling of via holes have been identified. One approach involves using a scanning argon-ion laser to locally decompose the polymeric layer and then subsequently plasma-etch to yield via holes. The second method involves direct ablation using an excimer laser. We propose to study the key process parameters of these two approaches, e.g., etching speed, hole geometry, formation, and removal of residual products process windows. laser wavelength, and damage to other circuit components. These parameters will be evaluated and optimized. Working samples will be prepared for interconnect metallization using the best identified approach.
3. Laser-patterned thick film photoresist: An alternate approach for interconnect metallization currently being developed for HDI applications is to laser-pattern a photoresist, followed by metallization. Key requirements in this approach are speed, resolution, and compatibility of resist development with other process steps. In addition, the resist must be easily removed without damage to other components. To date, a resist with all of the aforementioned requirements has not been identified. We propose to evaluate or modify commercial resists to develop a resist process compatible with the high-density interconnect approach. The work in this task will include a survey of available materials with potential utility.

Section 8
REFERENCES

1. R.J. Jense et al., IEEE 34th Electronic Components Conf., p. 73 (1985).
2. A.J. Blodgett, Jr., Sci. Amer., p. 86, July (1983).
3. P. Geldermans, IBM Tech. Disc. Bul., 25, 8, 4418 (1983).
4. T.F. Deutsch, D.J. Ehrlich, and R.M. Osgood, J. Appl. Phys., Lett. 35, 175, (1979).
5. D.J. Ehrlich and J.Y. Tsao, J. Vac. Sci. Technol., B-1, 969, (1983).
6. R. Solanki, C.A. Moore, and G.J. Collins, Solid State Technol., 220, (1985).
7. Y.S. Liu, C.P. Yakymshyn, H.R. Philipp, H.S. Cole, and L.M. Levinson, J. Vac. Sci Technol., B-3, (5), 1441, (1985).
8. D.J. Ehrlich et al., J. Vac. Sci. Technol., 21, 23 (1982).
9. D.K. Flynn et al., J. Appl. Phys., 59, 3914 (1986).
10. R.K. Montgomery, Appl. Phys. Lett., 48, 493 (1986).
11. T.T. Kodas et al., J. Appl. Phys., 62, 281 (1987).
12. G.J. Kisanick et al., J. Appl. Phys., 57, 1139 (1985).
13. R. Anderson and H. Taylor, J. Phys. Chem., 56, 498 (1952).
14. D.J. Ehrlich and J.Y. Tsao, Appl. Phys. Lett., 44, 267 (1984).
15. W.R. Wolf, R.E. Sievers, and G.H. Brown, Inorg. Chem., 11, 9, 1995 (1972).
16. F.A. Houle, C.R. Jones, T. Baum, C. Pico, C.A. Kovac, Appl. Phys. Lett., 46, 204, (1985).
17. C.R. Maylan, T.H. Baum, and C.R. Jones, Appl. Phys., A40, 1 (1986).
18. S.S. Eshildsen and G. Sorenson, Appl. Phys. Lett., 46 (1), 1101 (1985).
19. M.E. Gross, A. Applebaum and P.K. Gallagher, J. Appl. Phys., 61 (4), 1628 (1987).
20. W.G. Morris, W. Katz, H. Bakhru, A.W. Haberl, J. of Vac. Sci. Technol., (B) *3*, 391 (1985).
21. N. Feldstein, Plating, 803, Aug. (1970).
22. D.J. Sharp, Plating, 103, Aug. (1971).
23. H.R. Philipp and H. Ehrenreich, Phys. Rev., 129, 1550 (1963).
24. H.R. Philipp, D.G. Le Grand, H.S. Cole and Y.S. Liu, Polymer Engineering and Science, *27*, 15, 1148 (1987).
25. Y.S. Liu, D. Dentz and R. Beit, Opt. Lett., *9*, 76 (1983).
26. Y.S. Liu, J.P. Chernoch and W.B. Jones, Appl. Phys. Lett., 29, 32 (1976).

APPENDIX 1

ABSORBANCE SPECTRA OF ORGANOMETALLIC COMPOUNDS FOR LASER-ACTIVATED DEPOSITION STUDIES

FIGURE	COMPOUND
1	Dimethyl Cadmium (DMC) and Diethyl Telluride(DET) in Argon (10 cm path, 25 °C)
2	Chromium Carbonyl (2 cm path, 26 °C)
3	Molybdenum Carbonyl (2 cm path, 25 ,38 °C)
4	Copper hexafluoroacetylacetonate (2 cm path,70 °C)
5	Chromium hexafluoroacetylacetonate (2 cm path,70 °C)
6	Palladium hexafluoroacetylacetonate (2 cm path,60 °C)
7	Palladium Acetate on Quartz (0.1 μm film thickness)

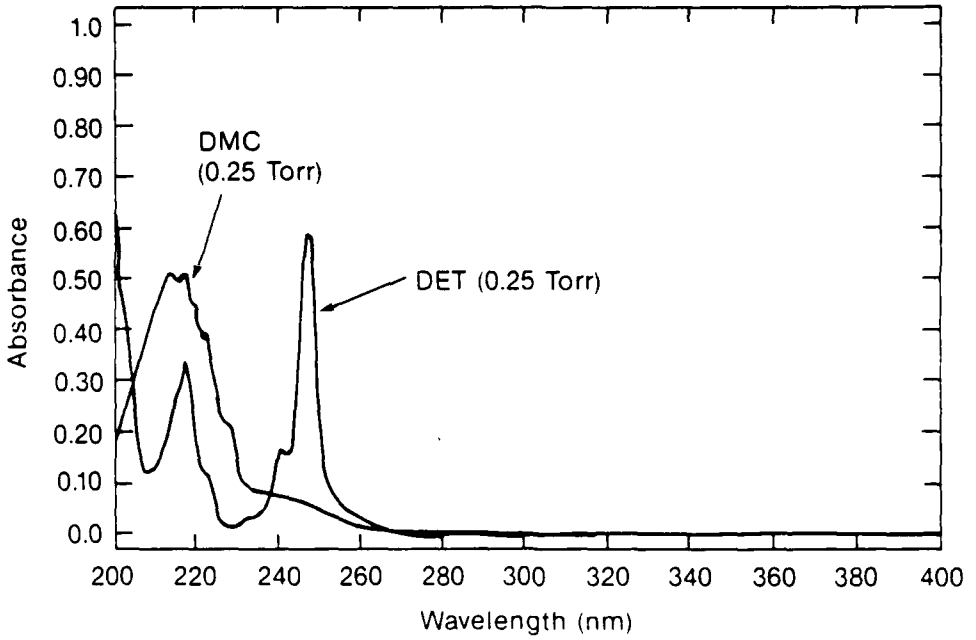

Fig AI-1 Absorption Spectra of DMC and DET in Argon (10 cm path, 25°C)

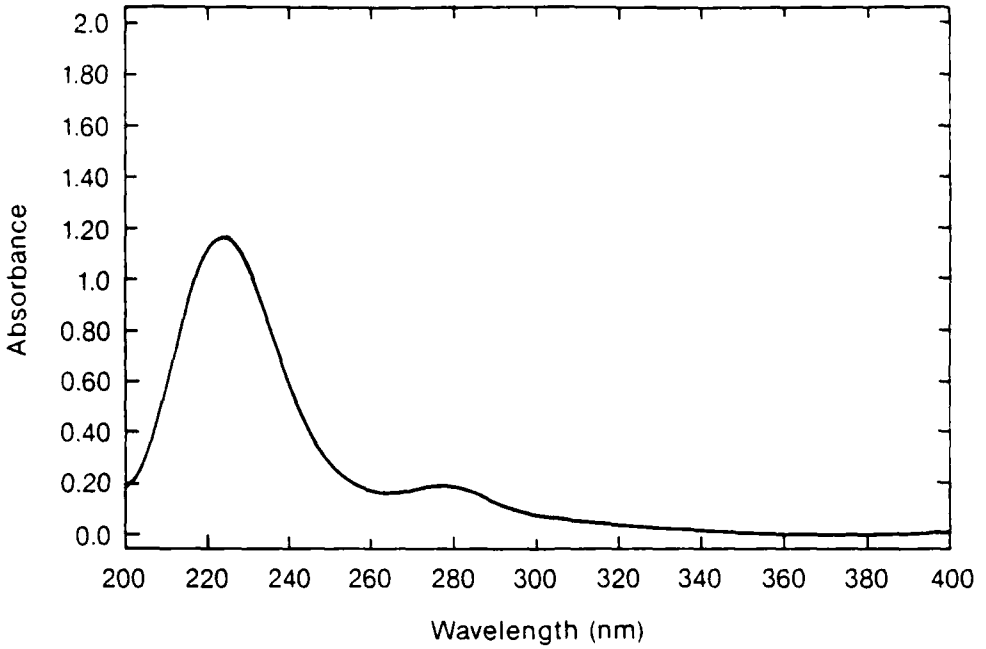

Fig. A1-2. Gas Phase Absorbance Spectra of Chromium Carbonyl (2 cm path, 26°C)

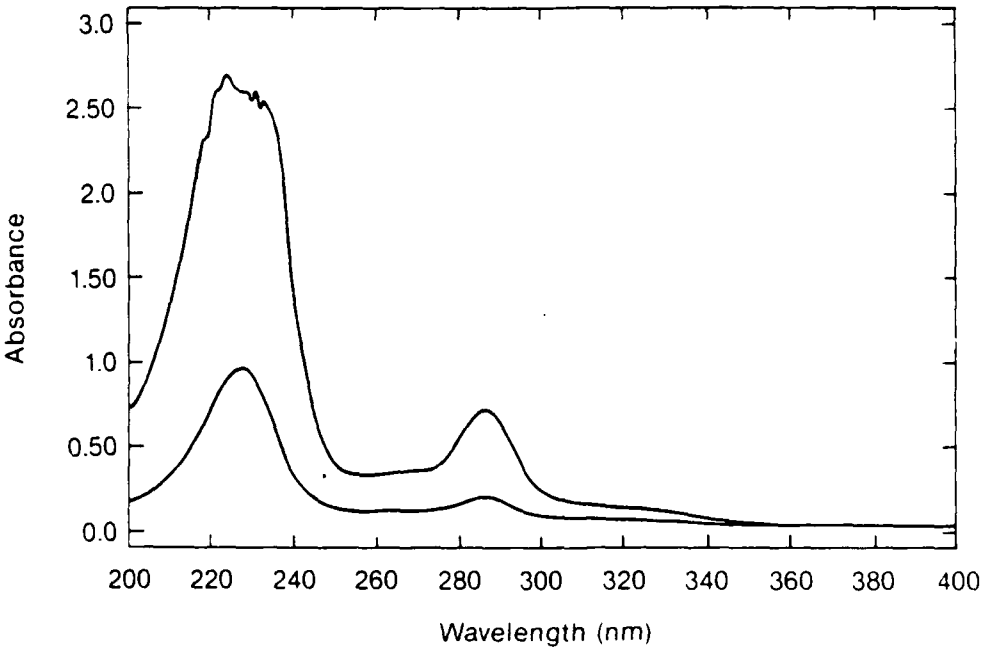

Fig A1-3. Gas Phase Absorbance Spectra of Molybdenum Carbonyl (2 cm path, 25°, 38°C)

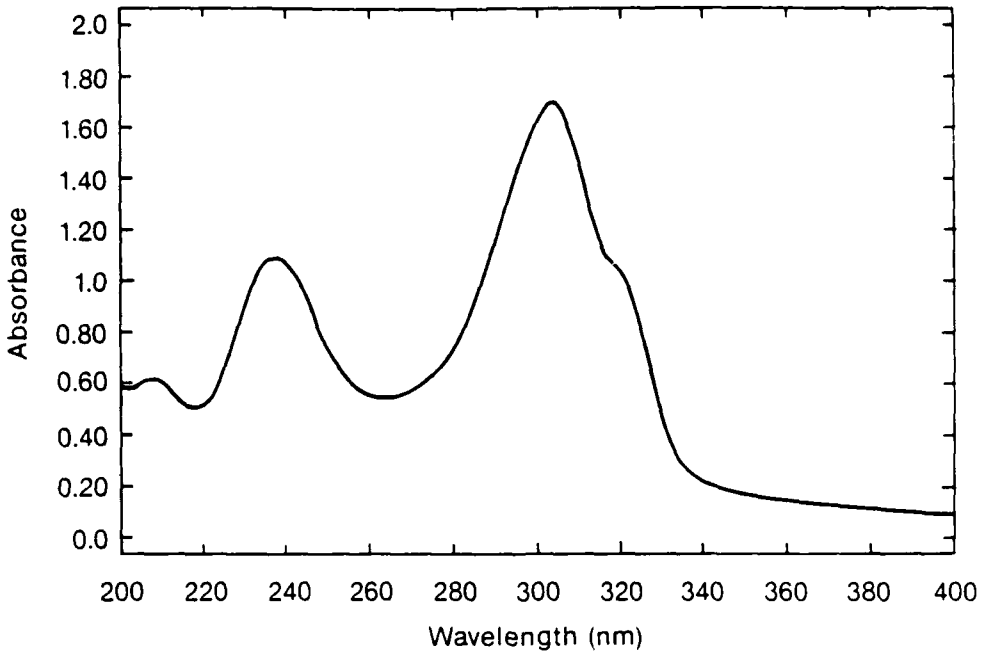

Fig. A1-4. Gas Phase Absorbance Spectra of Copper Hexafluoroacetylacetonate (2 cm path, 70°C)

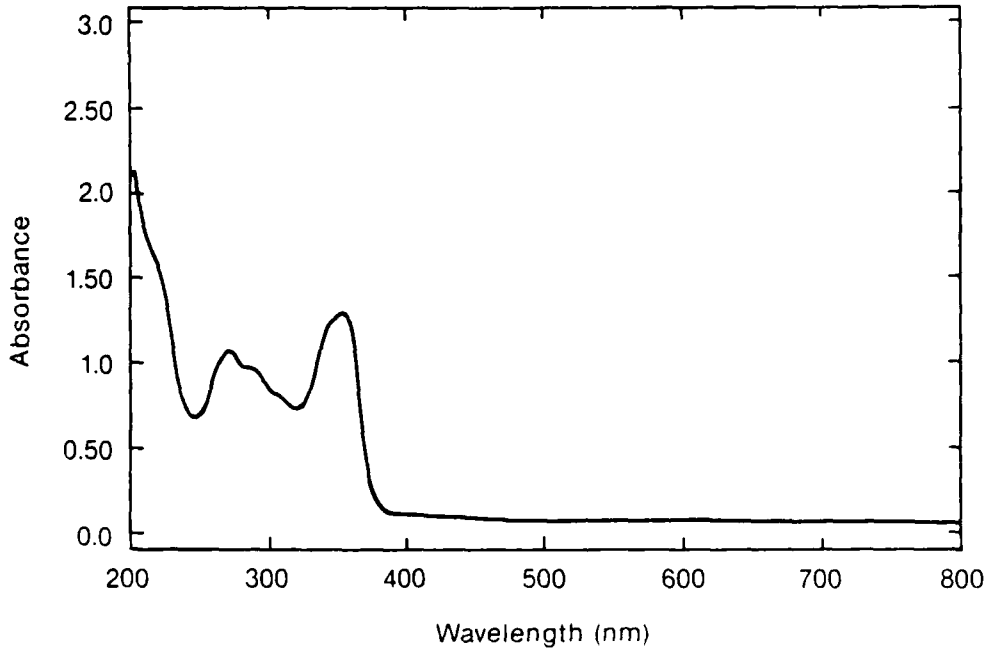

Fig. A1-5 Gas Phase Absorbance Spectra of Chromium Hexafluoroacetylacetonate (2 cm path, 70°C)

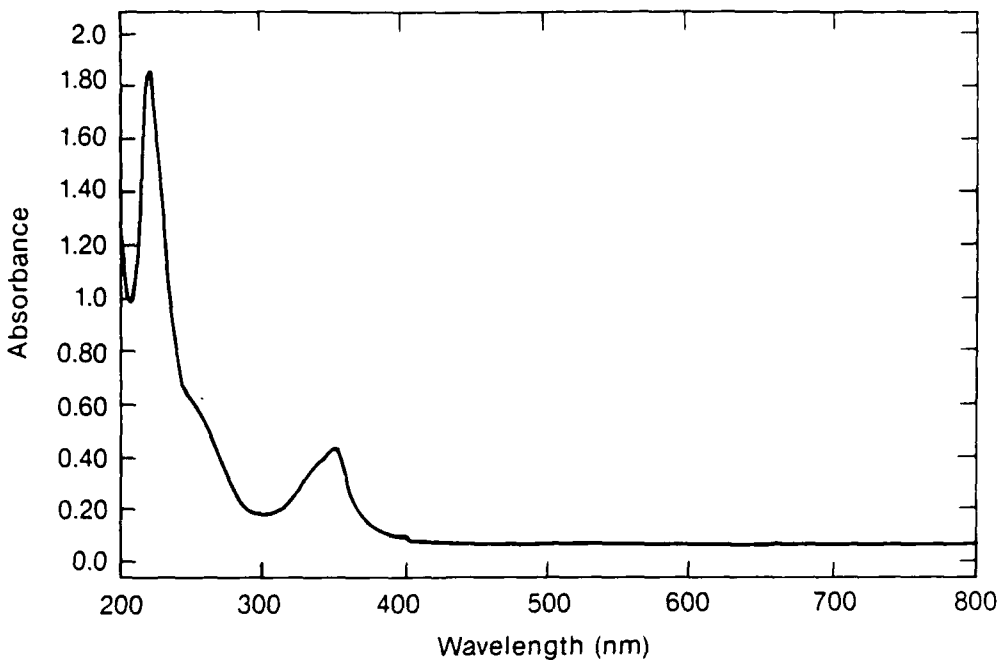

Fig A1-6. Gas Phase Absorbance Spectra of Palladium Hexafluoroacetylacetonate (2 cm path, 60°C)

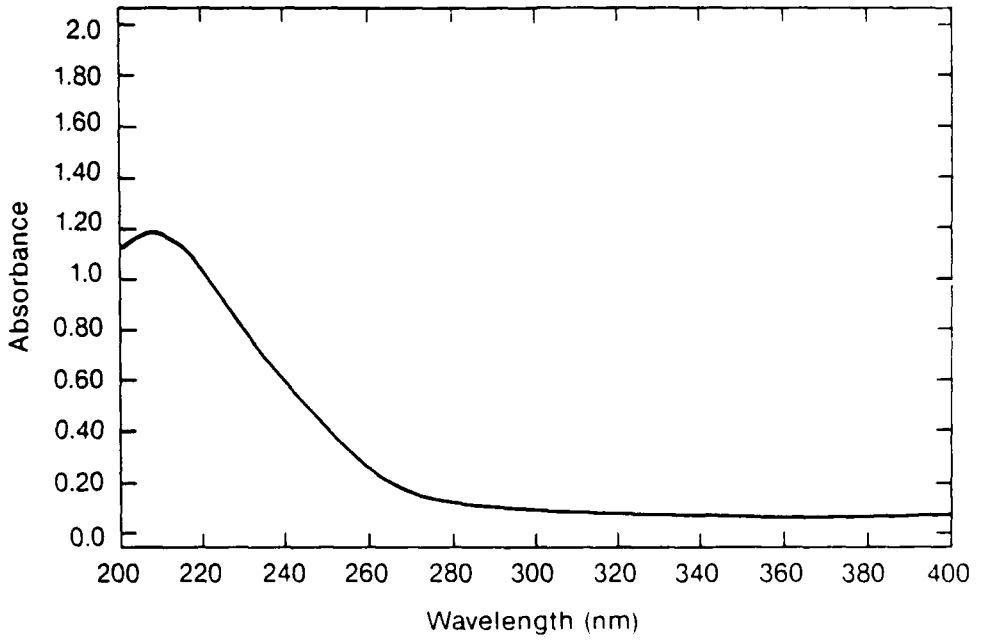

Fig A1-7. Gas Phase Absorbance Spectra of Palladium Acetate on Quartz (0.1 μm film thickness)

APPENDIX 2

SYNTHESIS OF ORGANOMETALLIC COMPOUNDS

1. SYNTHESIS OF COPPER BIS HEXAFLUOROACETYLACETONATE (Procedure adopted from J.A. Bertrand and R.I. Kaplan, Inorg. Chem. 5, 489 (1966))

   Copper nitrate (5.4 g) was dissolved in 50 ml H O. A solution of hexafluoroacetylacetone (9.36 g), sodium acetate (3.82 g) and 5 ml H O were added to the copper nitrate solution with mixing and the resultant precipitate filtered. This was recrystallized in a minimal amount of methanol to yield 3.4 g of pure copper bis hexafluoroacetylacetonate. The green crystals were stored in a vacuum dessicator with sulfuric acid and slowly converted to the dehydrated form resulting in blue crystals with the literature melting point.

2. SYNTHESIS OF CHROMIUM TRIS HEXAFLUOROACETYLACETONATE (Procedure of R. E. Sievers, et al., Inorg. Chem, 1, 966 (1962))

   A mixture of chromium nitrate (2.0 g), hexafluoroacetylacetone (3.12 g) and 20 ml of ethanol were heated for 10 min at 80 °C while the ethanol was slowly taken near dryness. The precipitate was filtered and recrystallized in carbon tetrachloride to yield about 1 g of brownish-green crystals.

3. SYNTHESIS OF ALUMINUM TRIS HEXAFLUOROACETYLACETONE (Procedure adopted from Inorg. Chem., 1, 966 (1962))

   A mixture of aluminum nitrate (1.87 g), hexafluoroacetylacetone (3.12 g) and 20 ml of ethanol were heated to 80 °C while the ethanol was slowly taken near dryness. The precipitate was filtered and recrystallized in carbon tetrachloride to yield 1.75 g of product melting at 70 °C.

4. SYNTHESIS OF PALLADIUM BIS HEXAFLUOROACETYLACETONATE (Procedure adopted from Inorg. Chem., 5, 489 (1966))

   A mixture of Palladium nitrate (4.6 g), hexafluoroacetylacetone (4.16 g) and 80 ml of methanol were warmed to boiling for 15 min. The methanol concentration was allowed to come near dryness and this was then taken up in carbon tetrachloride, filtered hot, cooled and filtered. The resulting crystals (2.2 g) melted at 92-94 °C and sublimed to give yellow needles at about 70 °C.

5. SYNTHESIS OF COPPER BIS ETHYLACETOACETATE (Procedure adopted from Inorg. Chem., 5, 489 (1966))

   Fehlings solution was prepared by adding copper sulfate (3.4 g) to 50 ml of H O with 1 drop of sulfuric acid. A 1:1 ammonia solution was then added dropwise until the initial precipitate formed was redissolved. Ethyl acetoacetate (3.3 g) was added to the above with stirring and the blue-green precipitate formed was filtered and washed with H O and dried. The product was recrystallized in methanol. The material thermally decomposed to copper metal at about 210 °C and started to sublime at 160 °C.

APPENDIX 3

OPTICAL PROPERTIES OF POLYIMIDE

When this program began, after extensive literature search, we found only scattered data available on optical properties of polymers. UV optical properties of polyimide-type materials are particularly lacking. In a separate internally funded program, we initiated a study to investigate UV optical properties of a variety of polymers of interest including poly(methyl)-methacrylate (PMMA), poly(vinylacetate) (PVA), poly(a-methyl styrene) (PS), poly(tetrafluoroethylene) (PTFE), polypropylene, nitrocellulose, copolymer styrene alcohol, polycarbonate and polyimide. In the following section, we describe some of the results obtained from this investigation. In particular, UV and near UV properties of a polyimide-type polymer, Ultem, (Tradename of GE) are discussed in details.

The absorption coefficient, α, of Ultem (Tradename of GE polyimide) resin was determined from transmission measurement using

$$I(x) = I_o \exp(-\alpha x)$$

where $I(x)$ and I_o are the transmitted and incident intensity and x is the sample thickness. The incident intensity was corrected for reflection losses and where appropriate, substrate absorption. These results are shown in Figures A-1 and A-2. A variety of samples were measured including bulk material of thickness 0.01 to 0.3 cm, thin sheets of thickness 25 to 100 μm, spin-coated films on quartz substrates of thickness 0.1 to 5 μm, and free-standing films of approximate thickness 0.1 to 0.8 μm. These last-mentioned samples were prepared by dissolving small pieces of polymer resin in 1,2,3,trichloropropane and putting a drop of this solution on a clean wafer surface. The solvent was allowed to evaporate and then the film was picked up on a wire ring of 2 to 3 in. diameter. The absence of an

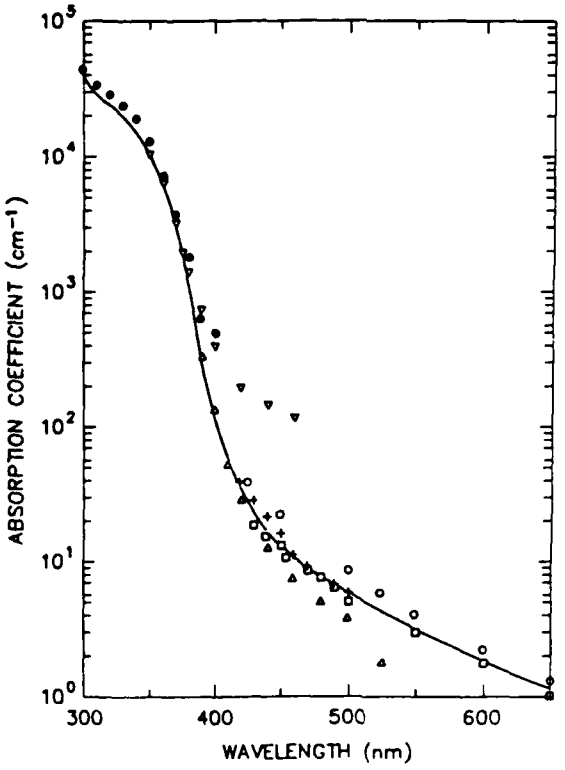

Figure A-1. Absorption coefficient vs. wavelength for Ultem™ (300 to 650 μm).

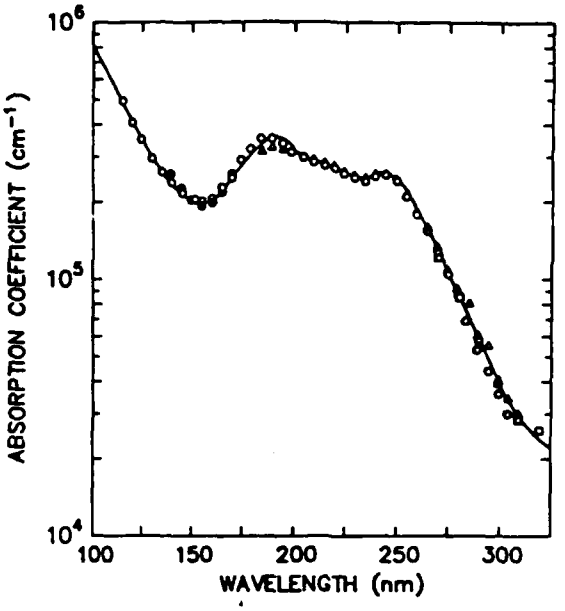

Figure A-2. Absorption coefficient vs. wavelength for Ultem™ (100 to 350 μm).

absorbing substrate enabled measurements on these samples to be made down to wavelength range of 105 nm and these results are mainly shown in Figure A-2. The vacuum monochromator used in these measurements has been described elsewhere (Ref. 23). The thickness of these samples was only estimated and was set by matching to other data at longer wavelengths. Hence, the fit of these data to results for wavelength greater than 200 nm was made arbitrarily good. In the region from 200 nm to 700 nm all data was obtained on a Hewlett-Packard model 8450A UV/Vis spectrophotometer. Reflectance measurements at near normal incidence were obtained on bulk polymer surfaces and results in the range 300 nm to 105 nm for two representative samples are shown in Figure A-3. The data are characterized by a maximum near 255 nm, an infection near 225 nm, a small peak at 195 nm, and a deep minimum at 165 nm. The uncertainty in these measurements is about 10%. When absorption coefficients are above 10^5 cm^{-1}, this measurement only examines the outer 100 nm surface of the sample. Other than for an alcohol rinse, the reflectance was measured on the sample as received with no polishing or other surface treatments.

Curves of absorption coefficients and reflectance versus wavelength were constructed from the data of Figures A-1 through A-3, and the Kramers-Kronig integrals given by Figures A-1 and A-2 were used in an iterative process to achieve a self-consistent set of optical parameters, which best agree with the experimental absorption and reflectance data, which are physically correct in the extrapolated region for wavelength less than 105 nm, and which yield values of n in the visible and agree with the independently obtained refractometer measurements. This procedure has been described in some detail elsewhere (Ref. 24). The resulting values of n and k for the polymer are plotted in Figure A-4. To facilitate the use this information the results are tabulated in Table A-1.

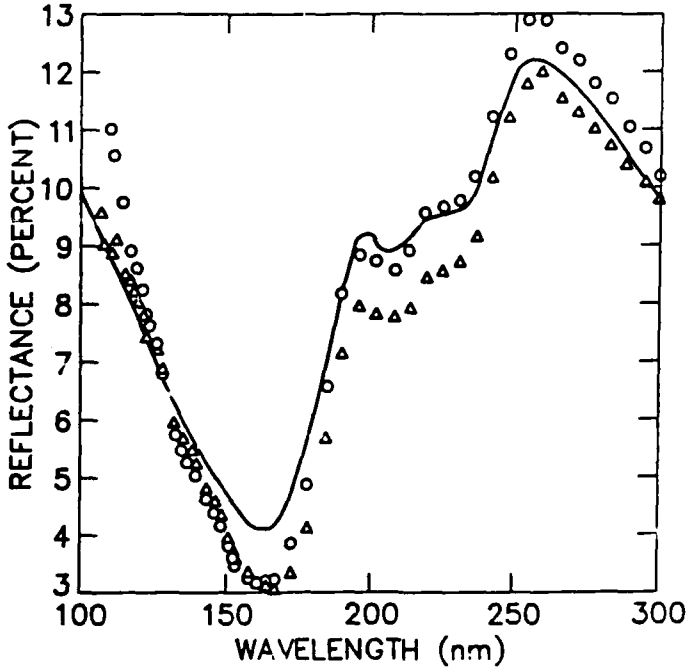

Figure A-3. Reflectance vs. wavelength of Ultem™ (100 to 300 μm).

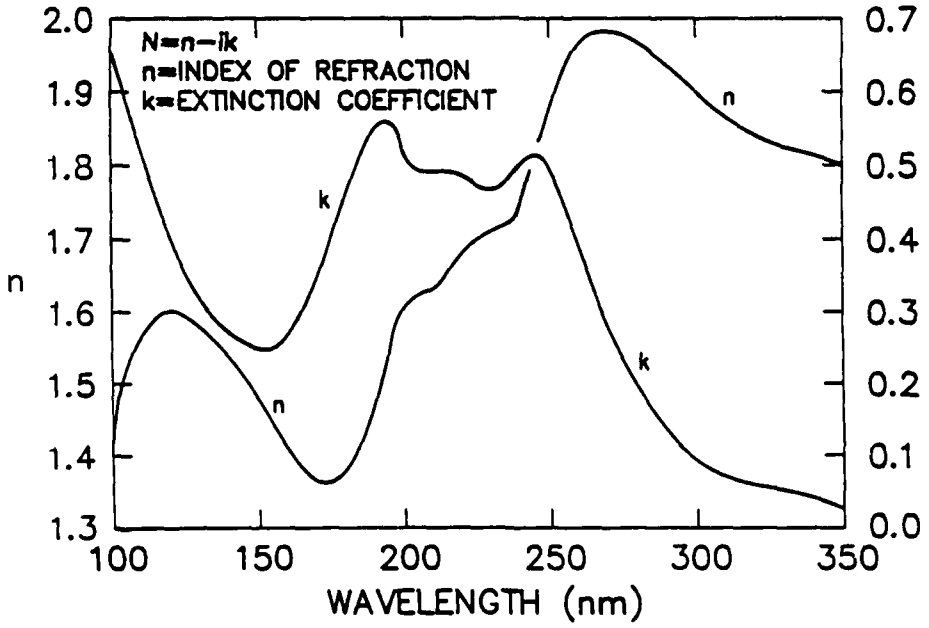

Figure A-4. Index of refraction and extinction coefficient vs. wavelength for Ultem™ (100 to 350 μm).

Table A-1

INDEX OF REFRACTION, EXTINCTION COEFFICIENT AND REFLECTANCE VALUES AT VARIOUS WAVELENGTHS FOR ULTEM™

Index of Refraction, n, Extinction Coefficient, k, and Reflectance, R, of Ultem(R) Polyetherimide Resin as Determined by Kramers-Kronig Analysis of Experimental Reflectance and Absorption Data

λ (nm)	n	k	R (%)
420.0	1.719	0.000131	6.99
400.0	1.735	0.000359	7.23
390.0	1.746	0.000946	7.39
380.0	1.760	0.00308	7.58
370.0	1.775	0.00835	7.81
360.0	1.791	0.0174	8.04
350.0	1.805	0.0298	8.25
340.0	1.817	0.0429	8.44
330.0	1.829	0.0537	8.62
320.0	1.846	0.0616	8.87
310.0	1.872	0.0721	9.28
300.0	1.908	0.0966	9.84
290.0	1.944	0.143	10.49
280.0	1.975	0.201	11.15
270.0	1.988	0.291	11.7[illegible]
260.0	1.965	0.397	12.17
255.0	1.930	0.458	12.22
250.0	1.872	0.503	11.92
245.0	1.804	0.519	11.27
240.0	1.748	0.503	10.42
235.0	1.721	0.477	9.79
230.0	1.712	0.471	9.61
225.0	1.701	[illegible]	9.[illegible]
220.0	1.681	[illegible]	9.[illegible]
215.0	1.655	0.496	9.29
210.0	1.63[illegible]	[illegible]	8.9[illegible]
205.0	1.62[illegible]	[illegible]	8.91
200.0	1.60[illegible]	[illegible]	9.18
195.0	1.5[illegible]	[illegible]	9.[illegible]
190.0	1.573	0.550	8.19
185.0	1.415	0.509	7.08
180.0	1.381	0.451	5.93
175.0	1.366	0.403	5.15
170.0	1.365	0.348	4.45
165.0	1.382	0.302	4.1[illegible]
160.0	1.411	0.26[illegible]	4.1[illegible]
155.0	1.446	0.25[illegible]	4.3[illegible]
150.0	1.481	0.24[illegible]	4.3[illegible]
145.0	1.510	0.25[illegible]	5.1[illegible]
140.0	1.53[illegible]	0.27[illegible]	5.6[illegible]
135.0	1.55[illegible]	0.28[illegible]	5.4[illegible]
130.0	1.584	0.312	6.[illegible]
125.0	1.59[illegible]	0.3[illegible]	[illegible]
120.0	1.60[illegible]	[illegible]	[illegible]
[illegible]	[illegible]	[illegible]	[illegible]
[illegible]	[illegible]	[illegible]	[illegible]
[illegible]	[illegible]	[illegible]	[illegible]

APPENDIX 4

PUBLICATIONS AND RELATED WORK

Presented at SPIE Meeting, Optoelectronics and Laser Applications in Science and Engineering,
Los Angeles, CA, January, 1988
(to be published in Conference Proceeedings)

Laser processing for interconnect technology

H.S. Cole, Y. S. Liu, R. Guida, and J. Rose

GE Research and Development Center
PO Box 8, Schenectady, New York 12309

ABSTRACT

Laser processing of polyimide dielectric layers for use in high-density interconnect structures was studied. A pulsed excimer laser was used to photoetch via holes and a CW argon ion laser operating at 351 nm was used to selectively deposit catalytic amounts of palladium on polyimide. Subsequent immersion of the irradiated samples in an electroless copper solution resulted in selective copper deposition.

1. INTRODUCTION

For high-density interconnect technology, high-performance organic polymers are used as dielectric layers instead of conventional inorganic materials. These polymers (such as polyimides), applied by spinning or laminating, are used as the interlayer dielectric because of their high thermal stability (Tg>400 °C) and low dielectric constant (E≈3.2). Devices made using these materials show reduced capacitive coupling between metal interconnects, thus resulting in higher density packages. Several levels of metal and polymer can be used to accommodate power, ground, and signal inputs. Generally, standard metallization and photoresist processes have been used to make interconnects and etch via holes for contact from one metal layer to another. An alternate approach utilizing laser technology for hole drilling and metallization has inherent advantages such as selectivity and elimination of the need for resists; this approach is presented.

2. VIA HOLE FORMATION

Excimer laser photoetching of polymers has been shown to be a convenient, fast, selective method of producing fine patterns or holes in polymeric materials.[1-4] Numerous studies have shown that this ablation process is due to a combination of local heating, photochemistry, and bond breaking to produce volatile fragments.[5,6] Experimental data have shown that the photoetching rate is dependent on factors such as laser fluence, wavelength, structure, and absorption coefficient of the polymer at the irradiating wavelength. By appropriate adjustment of irradiating parameters, the absolute etch rate can be optimized.[7]

Typical etch rate data is shown in Figure 1. The depth of etched holes is measured as a function of fluence and number of pulses to calculate the etch depth per laser pulse. A linear plot of etch depth per pulse vs. laser fluence for three different polymers are shown. These polymers were chosen because they represent very different absorption coefficients.[8] Polyimide (PI) and poly(methyl)styrene (PS) are strong absorbers with absorption coeffficients of 4.2×10^5 and $8.0 \times 10^5 cm^{-1}$ at 193 nm. Polymethylmethacrylate (PMMA) is a weak absorber with an absorbtion coefficient of 2.0×10^3 cm, which requires many laser pulses to start ablation. All three show a linear dependence on the laser fluence. For practical applications, the fluence should be as high as tolerable without undue damage to underlying circuitry. Etching rates of a few tenths of a micron per pulse allow hole drilling through 10-μm polyimide in less than a second using a commercially available excimer laser.

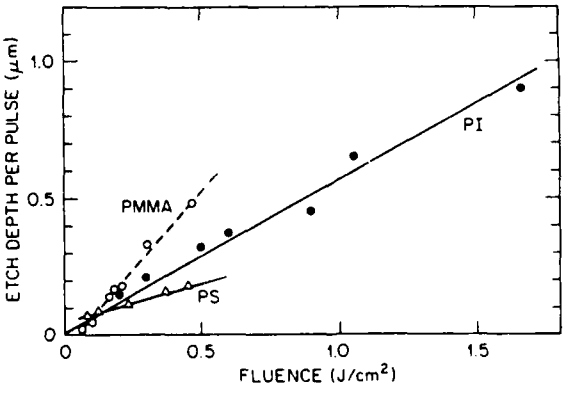

Figure 1 **Etch depth vs. laser fluence for three diferent polymers. The polyimide (PI) data is from Reference 8, while the polymethyl-methacrylate (PMMA) and poly(α-methyl) styrene (PS) data is from Reference 9.**

The hole profile can also be controlled by shaping the laser beam energy distribution. Since the etch rate is dependent on fluence, the edge profile of the hole can be adjusted appropriately. By varying the sample to mask spacing, it has been shown that the taper angle can be varied from 10° to 50°.[9] A laser drilled hole is shown in Figure 2. The sample is 10-μm-thick polyimide, which had been spin coated on silicon. During ablation, some residue is produced, which redeposits itself on the polyimide surface around the hole. This can be seen in Figure 2. This loosely held layer can be removed after laser irradiation and prior to additional processing sequences. Holes drilled in this manner and subsequently metallized showed good contact with underlying bonding pads.

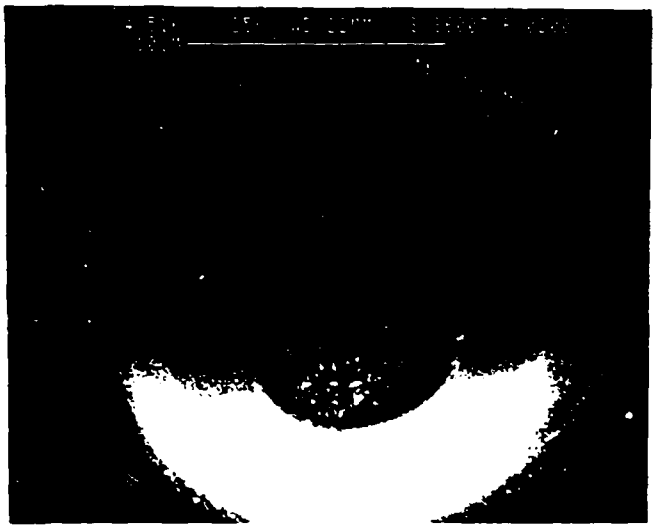

Figure 2 Excimer laser drilled via hole in 10-μm-thick polyimide film on silicon.

3. METAL DEPOSITION

Recently, laser-activated chemistry has been shown to be a viable method for fabricating metal lines on various substrates.[10-13] The production of metal lines by laser-induced deposition techniques offers several advantages over other thin film deposition processes. The laser process is non-contact, maskless, low-temperature, selective, and relatively simple. Pyrolysis and photolysis of organometallic compounds either in the gas phase or as thin adsorbed films have been studied using CW and pulsed lasers at a variety of wavelengths. Although numerous metals have been deposited on semiconductors and insulators using the laser activated process, little work has been reported on laser-induced selective metal deposition on polymeric materials. This area is particularly important for high-density, high-frequency interconnect assemblies and is the subject of our present study.

In general, the growth rate of laser activated deposition processes depends on beam intensity, wavelength, and concentration of precursors. The exact nature of the reaction is also extremely important. In gas phase photolysis, growth rates are limited by the transport of reactants and products to and away from the reaction zone. The proper laser wavelength must be used in order to couple the spectral properties of the gaseous phase compounds for photodissociation with efficient quantum yields. Although a variety of interesting photochemical reactions have been reported, none of these processes appear fast enough for line scanning applications.

The laser deposition rate is the rate of growth in thickness, V_g, and is related to the scan rate, V_s, via the following relationship, $V_s = D/d\ V_g$, where V_s is the scanning speed, V_g is growth velocity, D is beam diameter, and d is film thickness. Using a laser with a beam diameter of 10 μm to deposit a 1-μm-thick film requires a deposition rate (V_g) of 1 μm to scan at a rate of 10 μm and a deposition rate of 100 μm for scanning speeds of 1 mm/s. This is an important consideration for applications where fast laser scan rates are required.

In thermal processes, reactants of higher concentrations can be used because local heating of the substrate can occur without affecting the gas phase. As a result, several orders of magnitude improvement in growth rates have been achieved. In the case of thin layers of metal containing inks (metal or metal containing compounds dissolved in polymer), the growth rate is limited only by the film thickness, and offers high scanning speeds for direct writing applications. The approach used in this work was to laser decompose a catalytic amount of an organometallic palladium compound for subsequent immersion in an electroless copper plating solution. The advantage of this approach is that only a few monolayers of palladium atoms are needed and, hence, fast scan speeds are achievable.

In this work, using a CW argon ion laser at 351 nm as the exposure source, we have studied three different palladium compounds: palladium hexafluoro acetylacetonate (PdHFAcAc), palladium acetylacetonate (PdAcAc), and palladium acetate (PdAc). Each of these compounds has particular physical properties (Table 1) allowing us to evaluate the gas phase (e g, PdHFAcAc) as well as thin films (e.g., PdAcAc and PdAc) laser deposition.

Table 1
Palladium Compounds for Laser Deposition

COMPOUND	Pd CONTENT	SUBLIMATION TEMPERATURE (1)	DECOMPOSITION TEMPERATURE (2)	LASER DEPOSITION PROCESS
PALLADIUM (II) - HEXAFLUORO ACETYLACETONATE (Pd HFAc Ac)	20.4%	60°C	200°C	GAS PHASE
PALLADIUM (II) - ACETYLACETONATE (Pd Ac Ac)	34.7%	175°C	220°C	THIN FILM
PALLADIUM (II) - ACETATE (Pd Ac)	47.4%	200°C	220°C	THIN FILM

(1) FROM TGA DATA
(2) FROM DSC DATA

Experiments in the gas phase (PdHFAcAc) were carried out by placing a few milligrams of the palladium compound in a stainless steel cell fitted with a quartz window. The substrates were either polyimide films, which were spin-coated on glass from solution and fully cured, or 2-mil Kapton (polyimide) films laminated on glass. These samples were placed in the cell and the surface was irradiated through the quartz window using a focused laser beam. Prior to irradiation, the cell was evacuated and heated to a temperature of about 70 °C to give the desired vapor pressure. The vapor pressure was determined by extrapolation of the data published earlier on similar compounds, suggesting that at approximately 75 °C the vapor pressure is about 1 torr.[14] The gas pressure could be readily varied by adjustment of the cell temperature. The cell was positioned on an x-y translation stage and the laser power level and scan rate were computer controlled to allow a systematic study of deposition parameters. Less volatile palladium compounds were prepared on the polyimide surface by sublimation or by spin-coating from solution. The exposure to laser took place in air ambient without special arrangement. The advantage of this approach was that no special apparatus was needed during laser exposure.

At 351 nm, polyimide has an absorption coefficient of about 10^4 cm^{-1}, which results in 90% of the incident intensity being absorbed in the top 1-μm layer.[8] When a sample is exposed to a focused laser beam, local heating of the polymeric substrate causes thermal decomposition of the palladium compounds. Since polyimide is thermally stable to temperatures greater than 400 °C, and the palladium compounds studied decompose at about 225 °C, a process window is available where decomposition to palladium metal should occur without damage to the underlying polyimide. Photolytic decomposition of PdHFAcAc did not appear to be the dominant mechanism in gas phase laser irradiation. The gas phase absorbance spectra for this compound showed strong absorbance below 250 nm and a relatively weak band at 350 nm. Although we observed palladium deposition on quartz in the gas phase using a mercury vapor lamp as the exposure source, no significant deposition on quartz during laser irradiation was observed.

Results of laser irradiation of PdHFAcAc in the gas phase on polyimide substrates are summarized in Figure 3. After laser irradiation at the indicated power levels, the samples were immersed in an electroless copper solution. At low power levels, we see no palladium deposition (and hence no copper) because PdHFAcAc is sufficiently volatile to sublime off the surface during laser irradiation. Local heating caused deformation in the polyimide film, which was a spun-on polyimide (Pyralin 2540, Dupont Chemicals) on glass. Deformation was attributed to additional curing of polyimide (imidization, residual solvent loss, crosslinking) and was found to be extremely dependent on thermal history of the curing process. As the power level increased, laser energy was sufficient to locally decompose PdHFAcAc, resulting in subsequent electroless copper deposits. However, at these power levels, sufficient energy is available to damage the polyimide surface, thus resulting in copper deposits with poor morphology. The deposition rate depends on the vapor pressure as shown previously in the case of similar copper compounds,[15] which suggests higher gas cell temperatures would favor palladium deposition.

In subsequent experiments, less volatile compounds were used as adsorbed layers on polyimide for laser deposition. PdAcAc and PdAc were soluble in organic solvents and could be spin coated from solution to produce thin organometallic layers. Palladium acetate produced thin films that were amorphous, thus resulting in thin uniform coverage of polyimide.[16,17] Thermal decomposition of PdAc was used to determine catalytic effects of palladium on the electroless copper deposition on polyimide. Solutions of varying PdAc concentration were spun on polyimide and thermally decomposed (15 min at 250 °C). Using Rutherford Backscattering Spectroscopy (RBS), an optimum palladium surface concentration for electroless copper deposition was found to be about 5×10^{15} atoms/cm^2. At this surface concentration, smooth copper up to 1.25-μm thick was deposited with resistivity of several $\mu\Omega$ cm.

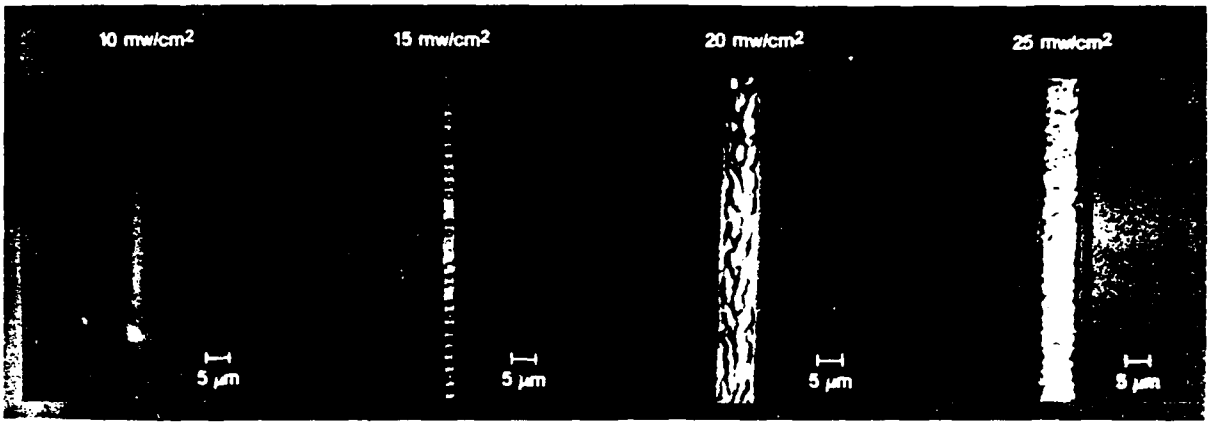

Figure 3 Laser deposition studies (351 nm, 32 mm/sec rate, polyimide substrate).

Laser deposition of PdAc on polyimide was found to yield similar results. RBS gave results similar to those for thermally decomposed material. A relatively large process window was available where smooth lines could be produced under a variety of power and scan conditions. These results are summarized in Figure 4. The beam diameter used in these experiments was measured to be 28 μm, which corresponds to fluence levels of 2 to 4×10^3 w/cm^2 for copper line deposits. As shown schematically in Figure 4, higher power levels caused thermal decomposition of polyimide. At these power and scan conditions, decomposed material is ablated off the surface (carrying away Pd and PdAc), resulting in no copper deposition. At lower power levels, smooth copper deposits are produced because local temperatures do not exceed the decomposition point of the polyimide film. By appropriate adjustment of the beam profile and PdAc concentrations, an optimum concentration of palladium deposition has yielded copper lines with smooth morphology.

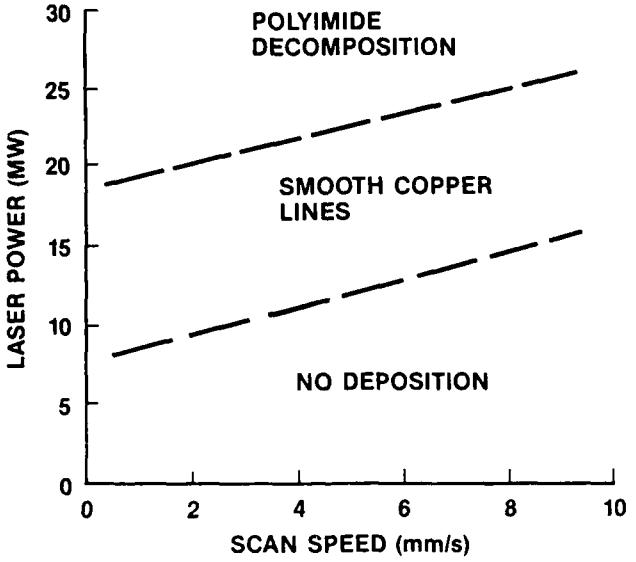

Figure 4 Power/scan speed relationships (PdAc on polyimide).

4. SUMMARY

Excimer laser drilling of via holes in polyimide has been demonstrated and is characterized by tapered side walls and drilling rates of a few tenths of a micron per pulse. For practical applications, via holes can be drilled in less than a second per hole. A direct writing technique using laser deposition of catalytic amounts of palladium followed by electroless copper deposition on polyimide has been demonstrated. Fast scanning rates of several cm/s were achieved. These processes provide a basis for laser-assisted metallization applicable to high-density interconnect technology.

5. ACKNOWLEDGMENTS

This work was supported in part by the Office of Naval Research through the SDI/IST office. The RBS analysis by Professor H. Bakhru of the State University of New York at Albany is gratefully acknowledged.

6. REFERENCES

1. R. Srinivasan and V. Mayne-Banton, *Appl. Phys. Lett. 41,* 576 (1982).
2. R. Srinivasan and W.J. Leigh, *J. Am. Chem. Soc. 104,* 6784 (1982).
3. J.E. Andrew, P.E. Dyer, D. Foster, and P.H. Key, *Appl. Phys. Lett. 43,* 717 (1983).
4. J.H. Brannon, J.R. Lankard, A.I. Baise, F. Burns, and J. Kaufman, *J. Appl. Phys. 58,* 2036 (1985).
5. R. Srinivasan and B. Braren, *J. Polymer Sci. 22,* 2601 (1984).
6. J.E. Andrew, P.E. Dyer, R.D. Greenough, and P.H. Key, *Appl. Phys. Lett. 43,* 1076 (1983).
7. H.S. Cole, Y.S. Liu, H.R. Philipp, and R. Guida, *Mat. Res. Soc. Symp. Proc. 72,* 242 (1986).
8. E. Sutcliffe and R. Srinivasan, *J. Appl. Phys. 60,* 3315 (1986).
9. H.S. Cole, Y.S. Liu, and H.R. Philipp, *Appl. Phys. Lett. 48,* 76 (1986).
10. H.R. Philipp, H.S. Cole, Y.S. Liu, and T.A. Sitnik, *Appl. Phys. Lett. 48,* 192 (1986).
11. J.T.C. Yeh and J.J. Donlon, *Elect. Chem. Soc.,* extended abstract, 87-2, 609, Fall Meeting (1987).
12. T.F. Deutch, D.J. Ehrlich, and R.M, Osgood, Jr., *Appl. Phys. Let. 35,* 175, 1979.
13. D.J. Ehrilich and J.Y. Tsao, *J. Vac. Sci. Technol. B-1,* 1969, 1983.
14. R. Solanki, C.A. Moore, and G.J. Collins, *Solid State Technol. 220,* June, 1985.
15. Y.S. Liu, C.P. Yakymyshyn, H.R. Philipp, H.S. Cole, and L.M. Levinson, *J. Vac. Technol. B-3* (5), 1441, 1985.
16. W.R. Wolf, R.E. Sievers, and G.H. Brown, *Inorg. Chem. 11* (9), 1995, 1972.
17. C.R. Moylan, T.H. Baum, and C.R. Jones, *Appl. Phys. A-40,* 1-5, 1986.
18. S.S. Eshildsen, and G. Sorenson, *Appl. Phys. Lett. 46* (1), 1101, 1985.
19. M.E. Gross, A. Applebaum and P.K. Gallagher, *J. Appl. Phys 61* (4), 1628, 1987.

Presented at Electrochemical Society Meeting, Symposium on Electronic Packaging,
Honolulu, Hawaii, October, 1987
(to be published in Conference Proceedings)

LASER-ACTIVATED COPPER DEPOSITION ON POLYIMIDE

H.S. Cole, Y.S. Liu, J.W. Rose, R. Guida, L.M. Levinson and H.R. Philipp
General Electric Company
Corporate Research and Development
P.O. Box 8
Schenectady, NY 12301

ABSTRACT

Laser irradiation of organometallic palladium compounds with a CW argon ion laser at 351 nm is used to selectively deposit catalytic amounts of palladium on polyimide. Subsequent immersion of the irradiated samples in an electroless copper solution results in copper deposition. Since a few monolayers of palladium are sufficient to catalyze the electroless copper process, fast writing speeds of several cm/s are obtained.

INTRODUCTION

Polymeric materials have desirable features as a packaging medium for VLSI, for multichip circuitry, and as an interconnect substrate. These materials are inexpensive, can be formed in any desired shape, can withstand required solder temperatures, have excellent dielectric strength, and, most importantly, have low dielectric constant, thus reducing capacitance coupling between metallization stripes. This capacitance often determines the ultimate speed or frequency limitation of packaged devices. For high-density packaging, a major concern is the interconnect layout. Many chips are mounted on a substrate and a complex interconnect scheme is required to contact different metal layers to each other and to other chips. Generally, standard metallization and photoresist processes have been used to make interconnects and etch via holes for contact from one metal layer to another.

Recently, laser-activated chemistry has been shown to be a viable method to fabricate metal lines on various substrates (1-4). The production of metal lines by laser-induced deposition techniques offers several advantages over other thin film deposition processes. The laser process is non-contact, maskless, low temperature, selective, and relatively simple. Pyrolysis and photolysis of organometallic compounds either in the gas phase or as thin adsorbed films have been studied using CW and pulsed lasers at a variety of wavelengths. A few examples of reported reactions are shown in Table 1.

The laser deposition rate is the rate of growth in thickness, V_g, and is related to the scan rate, V_s, via the following relationship;

$$V_s = D / d\, V_g$$

where

V_s = scanning speed
V_g = growth velocity
D = beam diameter
d = film thickness

Using a laser with a beam diameter of 10 μm to deposit a 1 μm thick film requires a deposition rate (V_g) of 1 μm/s to scan at a rate of 10 μm/s and a deposition rate of 100 μm/s for scanning speeds of 1 mm/s. This is an important consideration for applications where fast laser scan rates are required.

In general, the growth rate of laser activated deposition processes depends on beam intensity, wavelength, and concentration of precursors. The exact nature of the reaction is also extremely important. In gas phase photolysis, growth rates are limited by the transport of reactants and products to and away from the reaction zone. The proper laser wavelength must be used in order to couple the spectral properties of the gaseous phase compounds for photodissociation with efficient quantum yields. Although a variety of interesting photochemical reactions have been reported, none of these processes appear fast enough for line scanning applications.

In thermal processes, reactants of higher concentrations can be used because local heating of the substrate can occur without affecting the gas phase. As a result, several orders of magnitude improvement in growth rates have been achieved. In the case of thin layers of metal containing inks (metal or metal containing compounds dissolved in polymer), the growth rate is limited only by the film thickness, and offers high scanning speeds for direct writing applications. Although numerous metals have been deposited using laser activated chemistry, little work has been reported on discretionary writing on polymeric materials. This area is particularly important for high-density, high-frequency discretionary interconnect assemblies and is the subject of our present study.

EXPERIMENTAL

To achieve a useful laser metallization process on polyimide, fast scanning rates are required without adverse effects such as surface damage or resultant metal features with poor electrical and mechanical properties. The approach used in this work was to laser decompose a catalytic amount of an organometallic palladium compound for subsequent immersion in an electroless copper plating solution. The process is shown schematically in Figure 1. The advantage of this approach is that only a few monolayers of palladium atoms are needed and hence fast scan speeds are achievable.

In this work, using a CW argon ion laser at 351 nm as the exposure source, we have studied three different palladium compounds: palladium hexafluoro acetylacetonate (PdHFAcAc), palladium acetylacetonate (PdAcAc), and palladium acetate (PdAc). Each of these compounds has particular physical properties (Table 2) allowing us to evaluate the gas phase as well as thin film laser deposition.

Experiments in the gas phase (PdHFAcAc) were carried out by placing a few milligrams of the palladium compound in a stainless steel cell fitted with a quartz window. The substrates were either polyimide films, which were spin coated on glass from solution and fully cured, or 2-mil Kapton (polyimide) films laminated on glass. These samples were placed in the cell and the surface was irradiated through the quartz window using a focused laser beam. Prior to irradiation, the cell was evacuated and heated to a temperature of about 70 °C to give the desired vapor pressure. The vapor pressure was determined by extrapolation of the data published earlier on similar compounds, suggesting that at approximately 75 °C the vapor pressure is about 1 torr (11). The gas pressure could be readily varied by adjustment of the cell temperature. The cell was positioned on an x-y translation stage and the laser power level and scan rate were computer controlled to allow a systematic study of deposition parameters. Less volatile palladium compounds were prepared on the polyimide surface by sublimation or by spin-coating from solution. The exposure to laser took place in air ambient without special arrangement. The advantage of this approach was that no special apparatus was needed during laser exposure.

RESULTS

At 351 nm, polyimide has an absorption coefficient of about 10^4 cm^{-1}, which results in 90% of the incident intensity being absorbed in the top 1 μm layer (12). When a sample is exposed to a focused laser beam, local heating of the polymeric substrate causes thermal decomposition of the palladium compounds. Since polyimide is thermally stable to temperatures greater than 400 °C, and the palladium compounds studied decompose at about 225 °C, a process window is available where decomposition to palladium metal should occur without damage to the underlying polyimide. Photolytic decomposition of PdHFAcAc did not appear to be the mechanism in gas phase laser irradiation. The gas phase absorbance spectra for this compound is shown in Figure 2 (the cell path length was 2.5 cm). Strong absorbance below 250 nm and a band at 350 nm suggested potential photochemical decomposition. Although we observed palladium deposition on quartz in the gas phase using a mercury vapor lamp as the exposure source, no significant deposition on quartz during laser irradiation was observed.

Results of laser irradiation of PdHFAcAc in the gas phase on polyimide substrates are summarized in Figure 3. After laser irradiation at the indicated power levels, the samples were immersed in an electroless copper solution. At low power levels, we see no palladium deposition (and hence no copper) because PdHFAcAc is sufficiently volatile to sublime off the surface during laser irradiation. Local heating caused deformation in the polyimide film, which was a spun-on polyimide (Pyralin 2540, Dupont Chemicals) on glass. Deformation was attributed to additional curing of polyimide (imidization, residual solvent loss, crosslinking) and was found to be extremely dependent on thermal history of the curing process. As the power level increased, a point where sufficient energy was available to cause local decomposition of PdHFAcAc resulted in subsequent electroless copper deposits. However, at these power levels, sufficient energy is available to locally decompose the polyimide, thus resulting in copper deposits with poor morphology. The deposition rate depends on the vapor pressure as shown previously in the case of similar copper compounds (13) which suggests higher gas cell temperatures would favor palladium deposition. Although a fast scan rate of 32 mm/s was achieved with PdHFAcAc, complications of maintaining uniform cell temperatures caused us to conclude that more volatile palladium compounds were needed for gas phase deposition. Conversely, less volatile compounds could be used as adsorbed layers on polyimide since only a thin catalytic surface is required for electroless copper deposition.

Palladium acetylacetonate (PdAcAc) and palladium acetate (PdAc) were two other compounds with much lower vapor pressures. Both compounds were soluble in organic solvents and could be spin coated from solution to produce thin organometallic layers. Palladium acetate produced thin films that were amphorous, thus resulting in thin uniform coverage of polyimide (14,15). Thermal decomposition of PdAc was used to quantitatively study catalytic affects of palladium on the electroless copper deposition on polyimide. Solutions of varying PdAc concentration were spun on polyimide and thermally decomposed (15 min at 250 °C). Using Rutherford Backscattering Spectroscopy (RBS), an optimum palladium surface concentration for electroless copper deposition was found to be about 5×10^{15} atoms/cm^2 corresponding to an average value of a few monolayers of palladium. With this palladium surface concentration, smooth copper up to 1.25 μm thick was deposited with resistivity of several $\mu\Omega$ cm.

Laser deposition of PdAc on polyimide was found to yield similar results. RBS gave results similar to those for thermally decomposed material. A relatively large process window was available where smooth lines could be produced under a variety of power and scan conditions. These results are summarized in Figure 4. The beam diameter used in these experiments was measured to be 28 μm, which corresponds to fluence levels of 2 to 4×10^3 w/cm^2 for copper line deposits. As shown schematically in Figure 4, higher power levels caused thermal decomposition of polyimide.

At these power and scan conditions, decomposed material is ablated off the surface (carrying away Pd and PdAc) resulting in no copper deposition. At lower power levels, smooth copper deposits are produced because local temperatures do not exceed the 550 °C decomposition point of the polyimide film. By appropriate adjustment of the beam profile and PdAc concentrations, an optimum concentration of palladium deposition has yielded copper lines with smooth morphology.

In summary, a direct writing technique using laser deposition of catalytic amounts of palladium for subsequent electroless copper deposition on polyimide has been demonstrated and is potentially useful in packaging applications for high-density discretionary interconnects. Fast scanning rates of several cm/s were achieved. The thermal process has a low activation energy, allowing laser processing at low fluence levels. Laser-activated catalytic processes demonstrated in this work also offer interesting opportunities for metal deposition and patterning applications in microlithography.

ACKNOWLEDGEMENTS

This work was supported by the Office of Naval Research through the SDI/IST office. RBS analysis by Professor H. Bakhru of the State University of New York at Albany is gratefully acknowledged.

REFERENCES

1. T.F. Deutch, D.J. Ehrlich, and R.M, Osgood, Jr., *Appl. Phys. Let. 35,* 175, 1979.
2. D.J. Ehrilich and J.Y. Tsao, *J. Vac. Sci. Technol., B-1,* 1969, 1983.
3. R. Solanki, C.A. Moore, and G.J. Collins, *Solid State Technol. 220,* June, 1985.
4. Y.S. Liu, C.P. Yakymyshyn, H.R. Philipp, H.S. Cole, and L.M. Levinson, *J. Vac. Technol. B-3,* (5), 1441, 1985.
5. D.J Erlich et al., *J. Vac. Sci. Technol. 21* 23, 1982.
6. D.K. Flyn et al., *J. Appl. Phys. 59,* 3914, 1986.
7. R.K. Montgomery, *Appl. Phy. Lett. 48,* 493, 1986.
8. T.T. Kodas et al., *J. Appl. Phys. 62,* 281, 1987.
9. Y.S. Liu et al., *J. Vac. Sci. Technol. B3,* 1441, 1985.
10. G.J. Fisanik et al., *J. Appl. Phys. 57,* 1139, 1985.
11. W.R. Wolf, R.E. Sievers, and G.H. Brown, *Inorg. Chem. 11,* (9), 1995, 1972.
12. H.R. Philipp, H.S. Cole, Y.S. Liu, and T.A. Sitnik, *Appl. Phys. Lett. 48,* 192, 1986.
13. C.R. Moylan, T.H. Baum, and C.R. Jones, *Appl. Phys. A-40,* 1-5, 1986.
14. S.S. Eshildsen, and G. Sorenson, *Appl. Phys. Lett. 46* (1), 1101, 1985.
15. M.E. Gross, A. Applebaum and P.K. Gallagher, *J. Appl. Phys 61* (4), 1628, 1987.

Table 1

Direct Write Laser Metal Deposition Processes

PROCESS	REACTION	DEPOSITION RATE	SCAN RATE
GAS PHASE PHOTOLYSIS	$Cd(CH_3)_2 \xrightarrow[257\ nm]{(CW)} Cd$	1 μm/s [5]	TOO SLOW FOR LINE SCAN
THIN FILM PHOTOLYSIS	$Cr(CO)_6 \xrightarrow[308\ nm]{(PULSED)} Cr$	10^{-4} μm/s [6] (10 Hz)	
	$Mn_2(CO)_{10} \xrightarrow[325\ nm]{(CW)} Mn(CO)_5\cdot$ $Mn(CO)_5\cdot + Ag\ OTf \longrightarrow Ag$	10^{-3} μm/s [7]	
GAS PHASE PYROLYSIS	$(CH_3)_2\ Au(HFAc) \xrightarrow[514\ nm]{(CW)} Au$	6 μm/s [8]	~.1 mm/s
	$WF_6 + Si \xrightarrow[514\ nm]{(CW)} W$	100 μm/s [9]	~1 mm/s
THIN FILM PYROLYSIS	$Au\text{-ink} \xrightarrow[514\ nm]{(CW)} Au$	DICTATED BY [10] INITIAL FILM THICKNESS	>0.2 mm/s

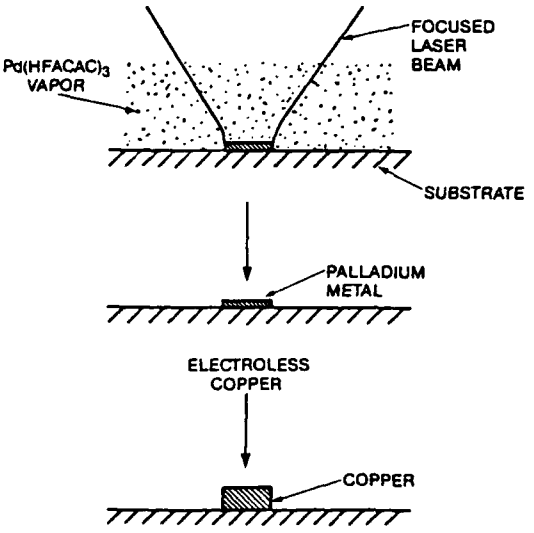

Figure 1. Laser-activated Copper Deposition Process

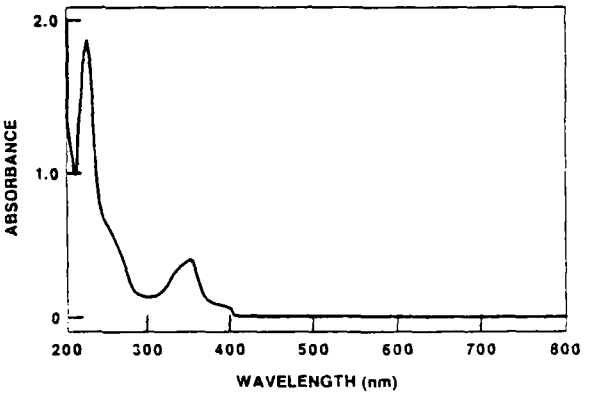

Figure 2. Gas Phase Absorbance Spectra of PdHFAcAc

Table 2
Palladium Compounds for Laser Deposition

COMPOUND	Pd CONTENT	SUBLIMATION TEMPERATURE (1)	DECOMPOSITION TEMPERATURE (2)	LASER DEPOSITION PROCESS
PALLADIUM (II) - HEXAFLUORO ACETYLACETONATE (Pd HFAc Ac)	20.4%	60°C	200°C	GAS PHASE
PALLADIUM (II) - ACETYLACETONATE (Pd Ac Ac)	34.7%	175°C	220°C	THIN FILM
PALLADIUM (II) - ACETATE (Pd Ac)	47.4%	200°C	220°C	THIN FILM

(1) FROM TGA DATA
(2) FROM DSC DATA

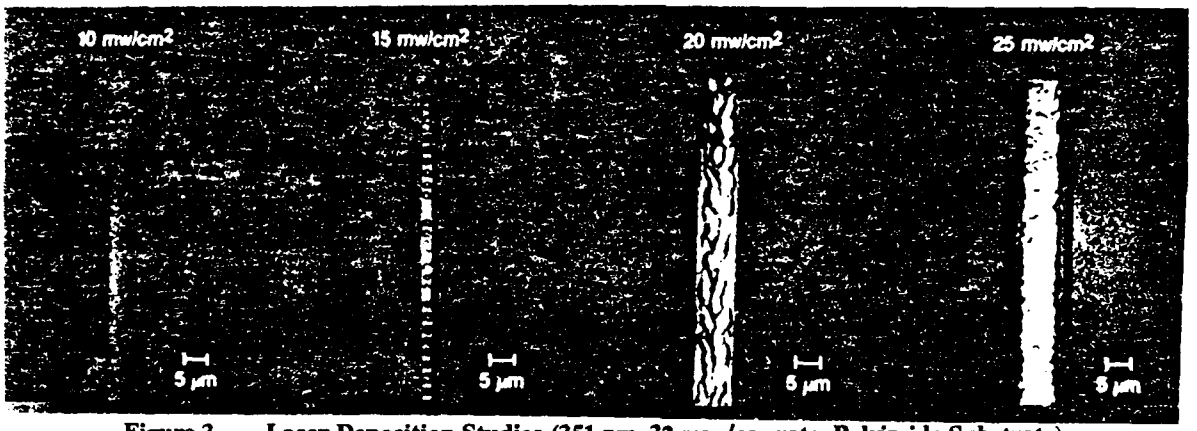

Figure 3. Laser Deposition Studies (351 nm, 32 mm/sec rate, Polyimide Substrate)

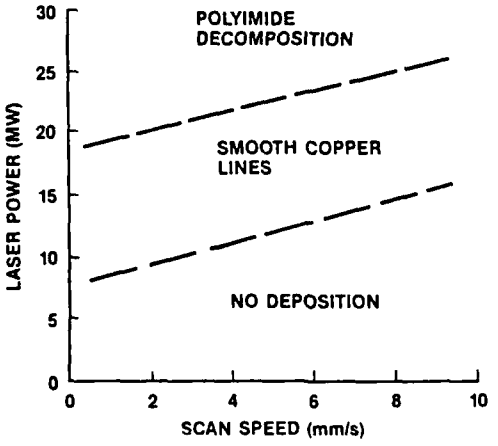

Figure 4. Power/Scan Speed Relationships (PdAc on Polyimide)

RELATED WORK

Publications/Reports/Presentations

I. Papers Published in Referenced Journals

1. "Dependence of photoetching rates of polymers at 193 nm on optical absorption depth," H.S. Cole, Y.S. Liu, and H.R. Philipp, Appl. Phys. Lett., 48, p. 76 (1986).
2. "Optical absorption of some polymers in the region 240-170 nm," H.R. Philipp, H.S. Cole, Y.S. Liu, and T.A. Sitnik, Appl. Phys. Lett, 48, p. 192 (1986).
3. "An X-ray photoelectron spectroscopy study of PMMA and PS surfaces irradiated by excimer lasers," M.C. Burrell, Y.S. Liu, and H.S. Cole, J. Vac. Sci. Technol., 4, p. 2459 (1986).
4. "Laser photoetching of polymers," H.S. Cole, Y.S. Liu, H.R. Philipp, and R. Guida, MRS Symp. Proceedings, Vol. 72, p. 241 (1986).
5. "Interactions of polymers with excimer lasers," Y.S. Liu, H.S. Cole, and H.R. Philipp, Proceedings of International Laser Sciences, American Physical Society (1987).
6. "Photoetching of polymers with excimer lasers, " SPIE, Vol. 774, p. 133 (1987).
7. H.R. Philipp, D.G. LeGrand, H.S. Cole, and Y.S. Liu, Polymer Engineering and Science, Vol. 27, 15, 1148 (1987).

II. Technical Reports (GE Internal)

1. "Photoetching of polymers with excimer lasers," Y.S. Liu, H.S. Cole, H.R. Philipp, and R. Guida, 87CRD088, May 1987.
2. "Power Chip Mosaics, A Discretionary Interconnect Method for Making Large Power Chips," A.J. Yerman, J.G. McMullen, and H.S. Cole, 87CRD147, July 1987. "Theory of Photoetching of Polymers," G. Mahan, H.S. Cole, Y.S. Liu, and H.R. Philipp, 87CRD210, October 1987.

III. Presentations

1. "Laser-Patterning of Polymers for Electronic Packages," H.S. Cole, Y.S. Liu, H.R. Philipp, and L.M. Levinson, 3rd U.S. /Japan Seminar on Dielectric and Piezoelectric Ceramics, Toyama, Japan, November 1986.
2. "Laser-Activated Copper Deposition on Polyimide," H.S. Cole, Y.S. Liu, J.W. Rose, R. Guida, L.M. Levinson, and H.R. Philipp, Symposium on Laser Processes for Microelectronic Applications, Electrochemical Society Meeting, Honolulu, Hawaii, October 1987.
3. "Power Chip-Mosaics," A.J. Yerman, J.G. McMullen, and H.S. Cole. GE GOSAM Power Electronics Meeting, Erie, PA, October 1987.
4. "High Density Interconnects for Electronic Packaging," R.O. Carlson, C.W. Eichelberger, L.M. Levinson, J.G. McMullen, C.A. Neugebauer, and R.J. Wojnarowski, SPIE Meeting, Optoelectronics and Laser Applications in Science and Engineering, Los Angeles, CA, January 1988).

BASIC DISTRIBUTION LIST

Technical and Summary Reports 1988

Organization	Copies
Defense Documentation Center Cameron Station Alexandria, VA 22314	12
Office of Naval Research Dept. of the Navy 800 N. Quincy Street Arlington, VA 22217 ATTN: Code 1131	6
Naval Research Laboratory Washington, DC 20375 ATTN: Code 6000 Code 6300 Code 2627	1 1 1
Naval Air Development Center Code 606 Warminister, PA 18974 ATTN: Dr. J. DeLuccia	1
Commanding Officer Naval Surface Weapons Center White Oak Laboratory Silver Spring, MD 20910 ATTN: Library	1
Naval Oceans Systems Center San Diego, CA 92132 ATTN: Library	1
Naval Posgraduate School Monterey, CA 93940 ATTN: Mechanical Engineering Department	1
Naval Air Systems Command Washington, DC 20360 ATTN: Code 310A Code 5304B Code 931A	1 1 1
Naval Air Prop. Test Ctr. Trenton, NY 08628 ATTN: Library	1
Naval Construction Battallion Civil Engineering Laboratory Port Hueneme, CA 93043 ATTN: Materials Div.	1
Naval Electronics Laboratory San Diego, CA 92152 ATTN: Electron Materials Sciences Division	1
Naval Missile Center Materials Consultant Code 3312-1 Point Magu, CA 92041	1
Commander David Taylor Research Center Bethesda, MD 20084	1
Naval Underwater System Ctr. Newport, RI 02840 ATTN: Library	1
Naval Weapons Center China Lake, CA 93555 ATTN: Library	1
NASA Lewis Research Center 2100 Brookpart Road Leveland, OH 44135 ATTN: Library	1

Naval Sea System Command
Washington, DC 20362
ATTN: Code 05M 1
Code 05R 1

Naval Facilities Engineering Command
Alexandria, VA 22331
ATTN: Code 03 1

Scientific Advisor
Commendant of the Marine Corps
Washington, DC 20380
ATTN: Code AX:1:Oak Ridge, TN 37380 1

Army Research Office
P.O. Box 12211
Research Triangle Part, NC 27709
ATTN: Metallurgy & Ceramics Program 1

Army Materials and Mechanics Research Center
Watertown, MA 02172
ATTN: Research Programs Office 1

Air Force Office of Scientific Research/NE
Building 410
Bolling Air Force Base
Washington, DC 20332
ATTN: Electronics & Materials Science Directorate 1

NASA Headquareters
Washington, DC 20546
ATTN: Code RM 1

National Bureau of Standards
Gaithersburg, MD 20899
ATTN: Metallurgy Division 1
Ceramics Division 1
Fracture & Deformation Division 1

Defense Metals & Ceramics Information Center
Battelle Memorial Inst.
505 King Avenue
columbus, OH 43201 1

Metals and Ceramics Div.
Oak Ridge National Laboratory
P.O. Box X

Los Alamos Scientific Lab.
P.O. Box 1663
Los Alamos, NM 87544
ATTN: Report Librarian 1

Argonne National Laboratory
Metallurgy Division
P.O. Box 229
Lemond, IL 60439 1

Brookhaven National Laboratory
Technical Information Division
Upton, Long Island
New York 11973
ATTN: Research Library 1

Lawrence Radiation Lab.
Library
Building 50, Room 134
Berkely, CA 1

David Taylor Research Ctr
Annapolis, MD 21402-5067
ATTN: Code 281 1
Code 2813 1
Code 0115 1

Professor Harlan U. Anderson
University of Missouri-Rolla
107 fulton Hall
Rolla, MO 65401

Professor R. Buchanan
University of Illionois
Department of Ceramic Engineering
Urbana, IL 61801

Professor Roger Cannon
Rutgers University
College of Engineering
P.O. Box 909
Piscataway, NJ 08859

Dr. N. Eror
Oregon Graduate Center
19600 N.W. Walker Road
Beaverton, OR 97006

Professor D. W. Readey
Department of Ceramic Engineering
1314 Kinnear Road
Columbus, OH 43212

Dr. Gordon R. Love
Corporate Research, Development
and Engineering
Sprague Electric Co.
North Adams, Mass 01247

Dr. Sidney J. Stein
Electro-Science Laboratories
2211 Sherman Ave
Pennsauken, NJ 08110

John Piper
Union Carbide Corporation
Electronics Division-Components
Dept.
P.O. Box 5928
Greenville, SC 29606

Professor R. Vest
Purdue University
West Lafayeette, IN 47907

Dr. J. V. Biggers
Pennsylvania State University
Materials Research Laboratory
University Park, PA 16802

Professor Larry Burton
Virginia Polytechnic Institute
and State University
Blacksburg, VA 24061

Prof. Donald M. Smyth
Lehigh University
Materials Research Laboratory
Coxe Laboratory 32
Bethlehem, PA 18015

Dr. K. D. McHenry
Honeywell Ceramics Center
5121 Winnetka av., N.
New Hope, MN 55428

Dr. Lew Hoffman
Hoffman Associates
301 Broadway (US 1) Suite 206A
P.I. 10492
Riviera Beach, FL 33404

Roger T. Dirstine
Ceramics Research
Unitrode Corporation
580 Pleasant St.
Watertown, Mass 02171

John C. Constantine
Electronic Materials Systems
Englehard Industries Division
1 West Central Ave.
E. Newark, NJ 07029

Tack J. Whang
Technical Center
Ferro Corporation
7500 E. Pleasant Valley Road
Independence, OH 44131

Prof. L. E. Cross
The Pennsylvania State University
Materials Research Laboratory
University Park, PA 16802

Professor R. Roy
The Pennsylvania State University
Materials Research Laboratory
University Park, PA 16802

Dr. G. Ewell
MS6-D163
Hughes Aircraft Company
Centinela & Teale Streets
Culver City, CA 90230

Dr. J. Smith
GTE Sylvania
100 Endicott Street
Danvers, MA 01923

Mr. G. Goodman, Manager
Corporation of Applied Research
Group
Globe-Union Inc.
5757 North Green Bay Avenue
Milwaukee, WI 53201

Dr. Kim Ritchie
Vice President
Corporate Research Laboratory
AVX Corporation
P.O. Box 867
Myrtle Beach, SC 29577

Advanced Research Projects
Materials Science Director
1400 Wilson Boulevard
Arlington, VA 22209

W.B. Harrison
Honeywell Ceramics Center
5121 Winnetka Ave. N.
New Hope, MN 55428

Dr. P. L. Smith
Naval Research Laboratory
Code 6361
Washington, DC 20375

Dr. George W. Taylor
Princeton Resources, Inc.
P.O. Box 211
Princeton, NJ 08540

Professor R. buchanan
Department of Ceramic Engineering
University of Illinois
Urbana, ILL 61801

Director
Applied Research Lab
The Pennsylvania State Univ.
University Park, PA 16802

Army Research Office
Box CM, Duke Station
ATTN: Met. & Ceram. Div.
Durham, NC 27706

Dr. R. R. Neurgaonkar
Rockwell International
Science Center
1049 Camino Dos Rios
P.O. Box 1085
Thousand Oaks, CA 91360

Mr. J. D. Walton
Engineering Experiment Station
Georgia Institute of Technology
Atlanta, GA 30332

National Bureau of Standards
Inorganic Mats. Division
Washington, DC 20234

David C. Larson
Senior Research Engineering
Nonmetallic Materials and Composites
IIT Research Institute
10 West 35 St.
Chicago, ILL 60616

END

DATE

FILMED

8-88

DTIC